Journal of Structural Geology, Vol. 6, No. 6, pp. 617 to 638, 1984
Printed in Great Britain.

0191-8141/84 $03.00 + 0.00

S–C Mylonites

G. S. LISTER*

Department of Structural Geology, Institute for Earth Sciences, University of Utrecht, 3508, TA Utrecht, The Netherlands

and

A. W. SNOKE†

Department of Geology, University of South Carolina, Columbia, SC 29208, U.S.A.

(*Received 7 October 1983, accepted in revised form 26 March 1984*)

Abstract—Two types of foliations are commonly developed in mylonites and mylonitic rocks: (a) S-surfaces related to the accumulation of finite strain and (b) C-surfaces related to displacement discontinuities or zones of relatively high shear strain. There are two types of S–C mylonites. Type I S–C mylonites, described by Berthé *et al.*, typically occur in deformed granitoids. They involve narrow zones of intense shear strain which cut across (mylonitic) foliation.

Type II S–C mylonites (described here) have widespread occurrence in quartz–mica rocks involved in zones of intense non-coaxial laminar flow. The C-surfaces are defined by trails of mica 'fish' formed as the result of microscopic displacement discontinuities or zones of very high shear strain. The S-surfaces are defined by oblique foliations in the adjacent quartz aggregates, formed as the result of dynamic recrystallization which periodically resets the 'finite-strain clock'. These oblique foliations are characterized by grain elongations, alignments of segments of the grain boundary enveloping surfaces, and by trails of grains with similar *c*-axis orientations.

Examples of this aspect of foliation development in mylonitic rocks are so widespread that we suggest the creation of a broad class of S–C tectonites, and a deviation from the general tradition of purely geometric analysis of foliation and time relationships. Kinematic indicators such as those discussed here allow the recognition of kilometre-scale zones of intense non-coaxial laminar flow in crustal rocks, and unambiguous determination of the sense of shear.

INTRODUCTION

MYLONITES have two important properties: (a) they are usually rocks which mark the locus of a zone of intense non-coaxial deformation; and (b) during flow the matrix minerals of a mylonite (e.g. quartz) deform crystal-plastically. Two effects result because large strains are accommodated by the crystal–plastic behaviour of the matrix minerals of the mylonite: (a) the matrix minerals undergo extensive dynamic recrystallization, normally with the result that reduction in grainsize takes place and (b) strong patterns of preferred crystallographic orientation typically develop (e.g. quartz *c*-axis fabrics). These characteristics are so widespread that they are almost essential to the definition of a mylonite. There are, however, other aspects which need to be considered in the definition of mylonite (see Bell & Etheridge 1973), and there are complications: for example, superplastic mylonites need not develop strong crystallographic fabrics. Controversy has surrounded issues raised by each of the above points.

Cataclastic vs mylonitic rocks

Much of the criticism levelled at the above definition of a mylonite stems from an unfortunate failure to recognize evidence for crystalline plasticity in mylonites (Higgins 1971). Cataclastic processes are certainly involved during mylonitization, since although the matrix minerals deform via crystal–plastic processes, other minerals in the mylonite (e.g. feldspar) may deform in a brittle fashion. In extreme cases, cataclasis of individual grains or groups of grains occurs. Other processes also take place, for example sliding on grain boundaries, sliding on transient displacement discontinuities, and diffusional mass-transfer. However, since crystal–plastic deformation dominates, mylonites should not be regarded as cataclastic rocks.

The broad division of mylonitic rocks versus cataclastic rocks (Sibson 1975, 1977) may occasionally require sophisticated microstructural analysis before a definitive classification can be made, but the advantages of this terminology far outweigh the disadvantages.

Pure shear vs simple shear

Controversy has also surrounded questions concerning the type of flow involved in the production of a mylonite, centred on the issue as to whether or not mylonites exist that formed in zones involving strictly coaxial deformation. This controversy has been fueled by difficulties associated with determining the type of flow that has taken place in specific shear zones. Ambiguity could be resolved if it was possible to specify the magnitude of relative displacements across the boun-

*Present address: Bureau of Mineral Resources, Geology and Geophysics, P.O. Box 378, Canberra City, 2601 Australia.
†Present address: Department of Geology and Geophysics, University of Wyoming, Laramie, WY 82071, U.S.A.

daries of a mylonite zone, but evidence for relative displacement is usually only circumstantial. Fabric and microstructural studies are important in clarifying the situation, but extrapolation of small-scale observations to apply to the bulk scale is rarely straightforward, because heterogeneous deformation results in the movement picture varying in a complex way from place to place, and with time.

The present state of this controversy can be summarized as follows. (a) Mylonites which form by strictly coaxial deformation are scarce, and when encountered constitute a geological phenomenon worthy of further investigation. Mylonites which so form involve unusual boundary conditions, for example in the case of the quartzite unit that ballooned and stretched above the intruding Papoose Flat pluton (Sylvester & Christie 1968, Sylvester *et al.* 1978). (b) In many cases where it has been previously argued that 'flattening' or coaxial deformation has been involved in the production of mylonite, detailed fabric and microstructural studies have subsequently revealed unequivocal evidence for a zone of non-coaxial laminar flow. (c) Although it is theoretically possible to arrive at the so-called 'bulk' movement picture by detailed analysis of the variation of the mesoscopic movement picture (in space as well as in time) problems of challenging complexity are encountered when this is attempted in practice. Major shear zones commonly anastomose, in which case the large-scale movement picture is defined by a composite of movement zones (with both synthetic and antithetic senses of shear), which separate lenses of less deformed rock. The movement picture can be further complicated by large-scale folding.

The choice of models for the movement picture in individual shear zones is not limited merely to 'flattening' vs 'simple shear'. These two models have remained undeservedly the focus of attention. Flattening (i.e. axially symmetric shortening) is a term much misused, since it refers to a specific type of deformation that is only one of many possible strain paths that involves coaxial deformation. Progressive simple shear, on the other hand, is only one type of non-coaxial laminar flow, and a component of progressive pure shear may commonly be involved as well (Lister & Williams 1983).

Note that laminar flow can be defined as a flow accomplished primarily as the result of (relative) translation of material planes parallel to the stream lines. Non-coaxial laminar flow (Fig. 1) implies that progressive simple shear is an important component of the flow, rather than just bulk translation. Use of this term implies more than merely that the flow is 'not turbulent', as should be clear from the above definition, and use of this term to describe flow in major shear zones seems preferable to unwieldy (and incorrect) attempts at generalization, such as 'heterogeneous simple shear with a component of shortening across the shear plane'.

Complex strain histories can be involved when a shear zone broadens or narrows by rotating the bulk flow plane. Proponents of the notion that finite-strain trajectories can be used to elucidate the kinematics of particular shear zones are faced with the problem of how to distinguish between histories involving vorticity numbers greater than unity (Means *et al.* 1980), such as rotating simple shear; and histories involving combinations of progressive simple shear with additional pure shear across the shear zone (vorticity number less than unity). This is likely to be impossible without independent kinematic information, since identical patterns of finite-strain variation can be produced by markedly different movement pictures.

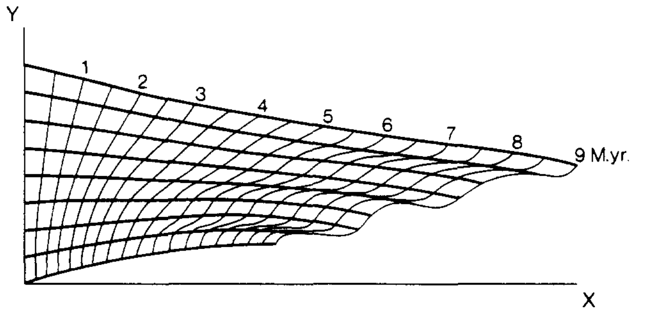

Fig. 1. A non-coaxial laminar flow that degenerates with time into narrow zones in which intense strains accumulate. Initially the strain is penetratively distributed. X–Y coordinates of points initially on the Y-axis are shown at different times. Heavy lines show trajectories of the points initially on the Y-axis.

The existence of a mylonite is itself not of great consequence, but it is important whether or not the mylonite marks the locus of a movement zone. Zones of intense (non-coaxial) laminar flow usually have fundamental tectonic significance. It is therefore important that structural geologists continue to develop techniques that allow such zones to be recognized. Fabric and microstructural studies are fundamental in this regard (for review see Simpson & Schmid 1983). Such studies also provide independent kinematic information concerning the evolution of such shear zones.

S–C MYLONITES

This paper is concerned with specific aspects of the way mylonitic foliation develops in zones of intense non-coaxial laminar flow, concentrating on a particular class of microstructures which we term type II S–C mylonites.

Type I S–C mylonites

The term S–C mylonite is derived from a nomenclature used by Berthé *et al.* (1979), who described the evolution of mylonites in an orthogneiss deformed in the South Armorican Shear Zone (France). Similar phenomena have been described by Jegouzo (1980) and Ponce de Leon & Choukroune (1980). These authors recognized two sorts of foliation: (a) S-surfaces related to the accumulation of finite strain; (b) C-surfaces related to localized high shear strains (where 'C' stands for 'cisaillement' or shear). In such rocks the mylonitic foliation anastomoses in and out of the zones of locally

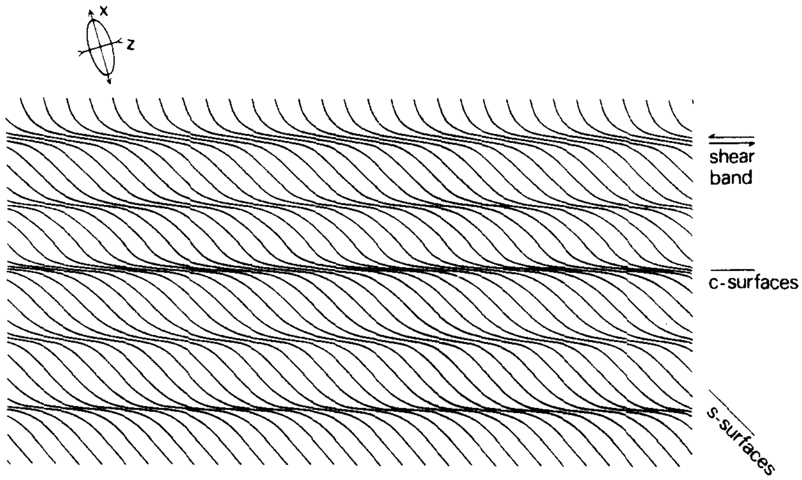

Fig. 2. Trajectories of the axis of principal finite extension in a type I S–C mylonite. Microstructures are characterized by shear bands transecting a mylonitic foliation. The S- and the C-surfaces are shown.

high shear strain in a way which is probably related to fluctuation of the intensity of finite strain (Fig. 2). Berthé *et al.* (1979) envisaged exact parallelism between schistosity and the local XY plane of the finite strain ellipsoid. For the purpose of this paper it is not important whether or not exact coincidence exists, providing there is some systematic relationship between foliation attitude and the local orientation of the XY plane of the finite strain ellipsoid.

According to Berthé *et al.* (1979), an important characteristic of an S–C mylonite is that the S- and the C-surfaces develop simultaneously. We do not think this restriction need be adhered to, since many type I S–C mylonites appear to have involved alternative histories of microstructural evolution. For example a well developed foliation defining the S-surfaces may have developed before localized yield and subsequent plastic deformation caused the formation of shear bands which define the C-surfaces. This type of behaviour is to be expected during non-coaxial laminar flow in which the velocity field degenerates with time as shown in Fig. 1, with shear strain concentrating in narrow zones towards the end of the history.

Rocks similar to the S–C mylonites described by Berthé *et al.* (1979) occur throughout the Cordilleran metamorphic core complexes in Arizona, California, and Nevada, U.S.A. and the S–C relationship can be used to determine the sense of shear in the major shear zones which occur in the upper levels of these complexes. Three alternative scenarios are applicable to the origin of such rocks: (a) synchronous development of mylonitic foliation and cross-cutting shear bands; (b) development of the narrow shear bands in late stages of the same deformation that produced the mylonitic foliation and (c) pre-existing fabric transected later by narrow shear bands.

The question of timing has been discussed thoroughly by Platt & Vissers (1980). In general it appears to be difficult to specify absolute timing relationships between S-surfaces and C-surfaces. However, occasionally, unequivocal timing criteria can be found, for example in the case when the metamorphic conditions change substantially between the periods when the S-surfaces and the C-surfaces are formed. For example the C-surfaces may be marked by specific reactions (e.g. biotite to chlorite, or muscovite to biotite). Vernon *et al.* (1983) examined the development of an S–C tectonite in a deformed granitoid, and concluded that the accumulation of finite strain first led to the development of a foliation (the S-surfaces) and later (ongoing) deformation led to the formation of cross-cutting shear bands and displacement discontinuities which define the C-surfaces. Vernon *et al.* (1983) therefore argued that an S_1–S_2 terminology was justified. However, there are problems associated with the use of an S_1–S_2 terminology. The difficulty is that, even if it can be shown that individual shear bands and displacement discontinuities did not form until (locally) the S-surfaces had developed, ongoing evolution of the microstructure is not precluded, nor is statistically coeval development of both foliations.

S–C relationships are extremely useful in that they draw attention to zones of non-coaxial laminar flow (when significant volume change can be ruled out). When field data suggest that the S- and C-surfaces are produced by ongoing deformation without significant change in the bulk movement picture, the exact details of the timing relationship may be of less significance than the S–C relationship itself.

Type I S–C mylonites have widespread occurrence in granites, granodiorites and augen gneisses subjected to mylonitization in shear zones.

Type II S–C mylonites

A second class of S–C mylonite develops in quartz-mica rocks subjected to mylonitization during conditions of decreasing pressure and temperature. The most characteristic microstructural features of type II S–C mylonites are mica 'fish' produced by boudinage and microfaulting of pre-existing (white) mica grains (Figs. 3 and 4). Individual mica 'fish' are linked by displacement discontinuities, and grain-scale zones of very high shear strain. These discontinuities and microshears are usually marked by trails of very fine-grained phyllosilicates, opaque minerals and occasionally fragmented feldspar grains. These trails define the C-surfaces.

The essential difference between type I S–C mylonites and type II S–C mylonites lies in the relative importance of the S- and C-surfaces. In type I S–C mylonites the S-surfaces are clearly discernible on the mesoscopic scale, anastomosing in and out of the narrow zones of high shear strain which define the C-surfaces. Furthermore, in most type I S–C mylonites, continuity is maintained across these narrow (ductile) shear zones. In type II S–C mylonites, on the other hand, the C-surfaces define the dominant mesoscopic foliation, and the S-surfaces are not always clearly discernible. Even on the microscopic scale, many C-surfaces in type II S–C mylonites appear to have involved transient displacement discontinuities.

In type II S–C mylonites the S-surfaces are not always as obvious as C-surfaces. Commonly they can be represented by foliations in the adjacent quartz aggregates, which form oblique to the C-surfaces. These foliations are defined by alignments of segments of the traces of the enveloping surfaces of the grain boundaries, elongate recrystallized grain shapes, and alignments of groups of similarly oriented recrystallized grains (Fig. 3). They appear to result because the quartz aggregate underwent (dynamic) recrystallization as shear movements took place, synchronously with the formation of the C-surfaces.

Such microstructures are spectacularly developed in quartz mylonites from the metamorphic core complexes of the western North American Cordillera (in Arizona, California and Nevada), in particular in the Coyote Mountains, SW of Tucson, Arizona (see acknowledgements), and from the Ruby Mountains, Nevada (Snoke 1980). Detailed studies have led to the conclusion that these microstructures are useful and consistent indicators of the sense of shear in rocks subjected to large-scale non-coaxial laminar flow, and their presence provides conclusive evidence that major shear zones are involved in the development of the Cordilleran metamorphic core complexes. More importantly, this is a class of microstructures in which the dominant foliation is related to shear surfaces, directly contradicting the view that foliations develop in exact relationships to the state of finite strain. We decided, therefore, to make a detailed fabric and microstructural study of type II S–C mylonites to characterize their properties.

Similar microstructures have also been recorded in mylonites from the axial zone of the Pyrenees, from the Seve–Köli thrust-slice complex in the Scandinavian Caledonides, from mylonites in various parts of the Alpine orogenic belt (e.g. mylonitic complexes in the Cycladic Archipelago, Greece), and from vertical shear zones in the Australian Precambrian (in retrograde shear zones in granulites of the Arunta complex in Central Australia). Hence type II S–C mylonites have widespread occurrence, and they form a valuable addition to the catalogue of kinematic indicators which a structural geologist can use to draw inferences concerning the movement picture.

MICA 'FISH'

Mica 'fish' form commonly in rocks where pre-existing large (white) mica grains are boudinaged by a combination of brittle and crystal–plastic processes (e.g. Eisbacher 1970). The remnant clasts are usually asymmetric in shape, and the (001) cleavage is either tilted back against the sense of shear (Fig. 5) or sub-parallel to the C-surfaces. In these orientations the easy slip plane in the mica lies in the extension field of the flow, and since the mica (001) is relatively strong, the clasts are relatively undistorted in these orientations. However, if the (001) plane of the mica is (even locally) tilted forward with respect to the C-surfaces, intense kinking, microfolding and/or cleavage fracturing results (Figs. 5i & j). The mica 'fish' are usually linked by trails of fragments, and when extensively developed, these trails commonly stair-step from one mica 'fish' to the next (Figs. 3 and 4). Each of the above microstructural characteristics is a useful kinematic indicator by itself.

The mechanisms by which mica 'fish' form can be inferred from microstructural observations, because the results of micro-boudinage can still be recognized, as well as evidence for the existence of displacement discontinuities in the flow field. The early developmental stages of a new mica 'fish' are occasionally preserved at a stage before the 'fish' has been separated from the host clast by a displacement discontinuity. As illustrated in Fig. 5, the host clast is transected by microfaults and microshears, which can form in either synthetic or antithetic relationships with the bulk shear sense. Different effects result, depending on the orientation of the (001) cleavage (Fig. 5). Notable amongst these are cleavage peels, through-cleavage microshears, and 'listric normal' faults. Note again that the (001) planes tend to be either parallel to the trails linking the 'fish' (i.e. the C-surfaces) or tilted back against the bulk shear sense.

One fairly intricate mechanism for the generation of mica 'fish' should be described in detail because it appears to have taken place in many of the different mylonites we have examined, and because it produces a distinctive shape of 'fish', which itself allows microstructural assessment of bulk shear sense, independent of other kinematic indicators. The mechanism is initiated by the formation of a 'listric normal' microfault, antithetic to the bulk shear sense, which first cuts down through the cleavage then curves into parallelism with it (Fig. 6a). The two segments are then drawn apart by continuing deformation, because the (001) plane lies in the extension field (Fig. 6b). Displacements on the curved microfault continue to be antithetic to the bulk shear sense, and because the fault is curved, the (001) planes in the new-formed segment rotate with respect to those of the host, as the two segments slide apart. A synthetic microshear or microfault is eventually responsible for the displacement discontinuity which causes the wide separation of the originally adjacent segments (Fig. 6c).

The most common mechanisms whereby 'fish' multiply are illustrated in Figs. 7 and 8. 'Listric normal' microfaults are found repeatedly in mica 'fish' in S–C mylonites (Fig. 8). Attention has already been drawn to the peculiar shape of mica 'fish' that results (Fig. 8a) and its usefulness as a reliable kinematic indicator.

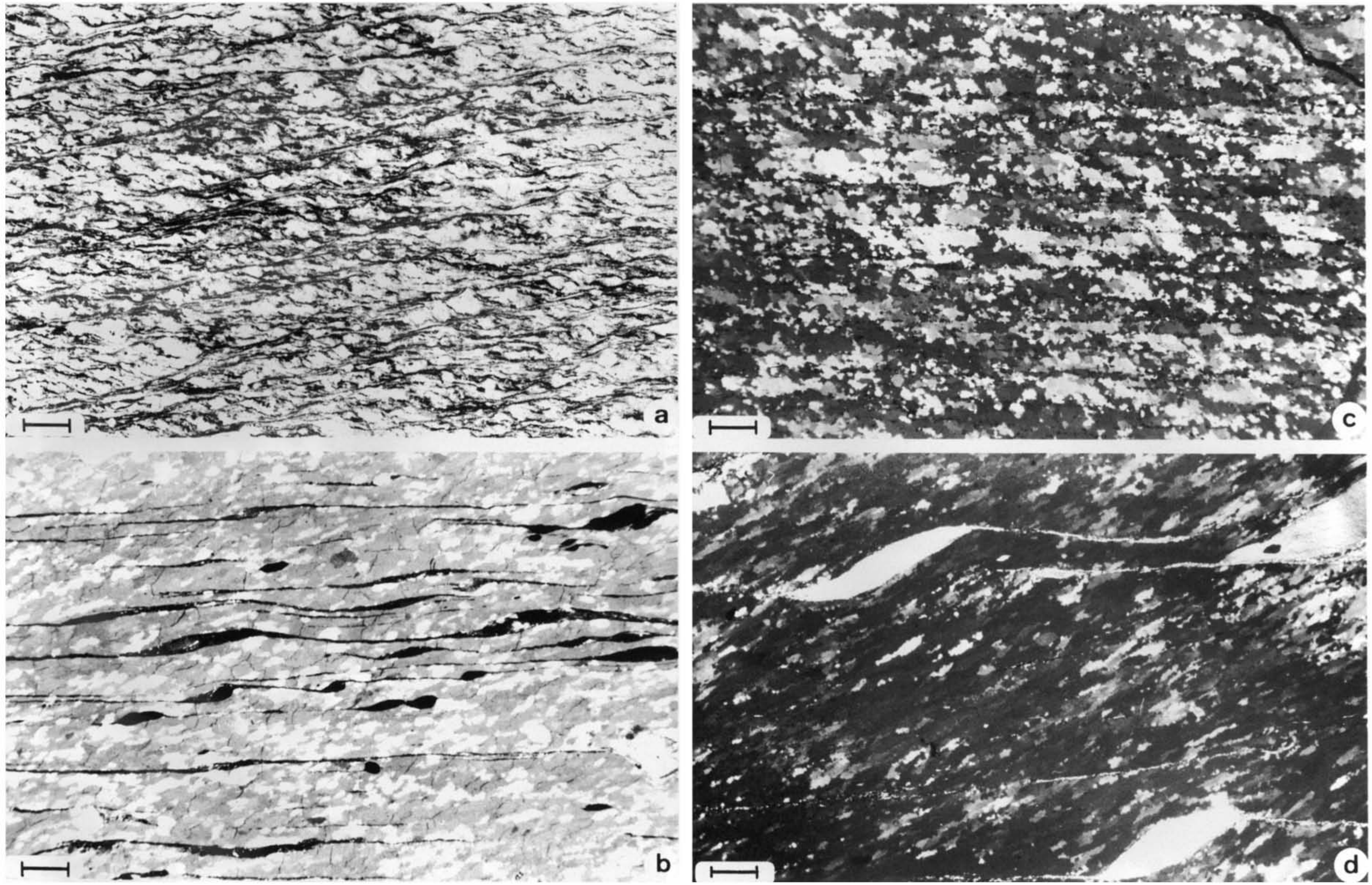

Fig. 3. Examples of the two types of S–C mylonite. (a) Typical type I S–C mylonite, from Palm Springs canyon, California. The mylonitic foliation anastomoses in and out of (sinistral) shear bands. (b) Typical type II S–C mylonite, Coyote Mountains, Arizona. Biotite and pyrite define 'fish' from which extend thin trails marking the locus of microscopic displacement discontinuities, or very narrow shear bands. These trails stair-step from one 'fish' to the next, indicating a dextral sense-of-shear. Note the oblique foliations in the adjacent dynamically recrystallized quartzite. (c) Type II S–C mylonite formed in an amphibolite-facies graphitic quartzite, Naxos, Cyclades, Greece. Migration recrystallization has led to conjugate grain-boundary alignments. The C-surfaces are defined by trails of opaques. Sense of shear is sinistral. (d) Type II S–C mylonite, Coyote Mountains, Arizona. Note that the mica (001) is approximately parallel to the oblique foliation in the dynamically recrystallized quartzite, and how the C-surfaces defined by trails extend across the section linking the mica 'fish'. Sense of shear is dextral. Scale bars are: (a) 8 mm; (b) 260 μm; (c) 290 μm; (d) 200 μm.

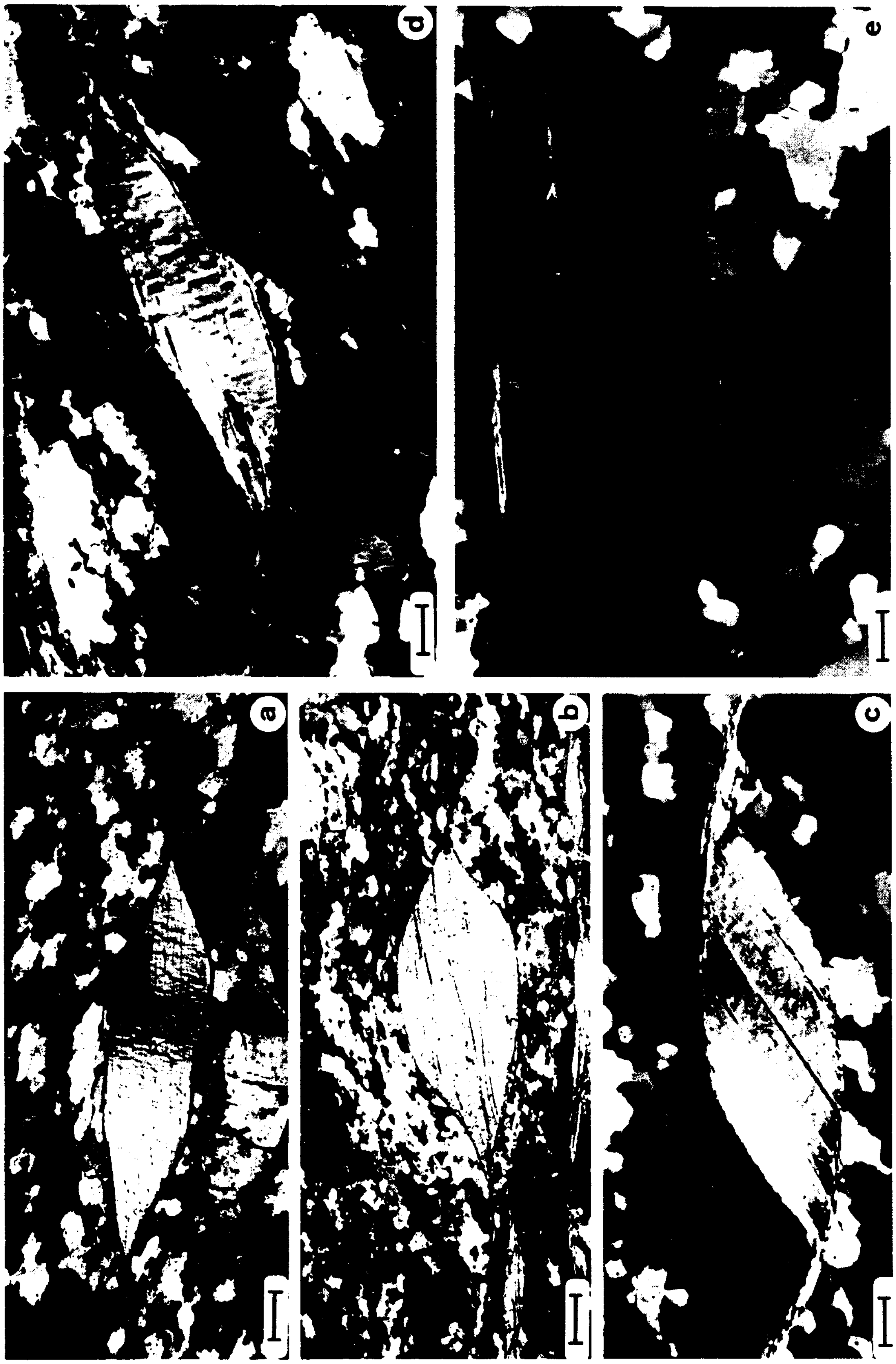

Fig. 4. Types of mica 'fish' found in type II S–C mylonites. The 'fish' in (a) and (b) have (001) only slightly inclined to the C-planes. The 'fish' in (c) and (d) have (001) tilted 30–40° back against the sense of shear, but note that the variation in shape is not entirely dependent on the orientation of (001). Long thin 'fish' with (001) parallel to the C-planes are also common (e). Examples (a) and (d) come from the Coyote Mountains, (b) and (c) from the Ruby Mountains and (e) from a recrystallized 'mylonite' in the Otztal massif, South Tirol. Sense of shear is dextral in (b), (c) and (d) and sinistral in (a). Scale bars are: (a) 80 μm; (b) 200 μm; (c) 40 μm; (d) 40 μm; (e) 40 μm.

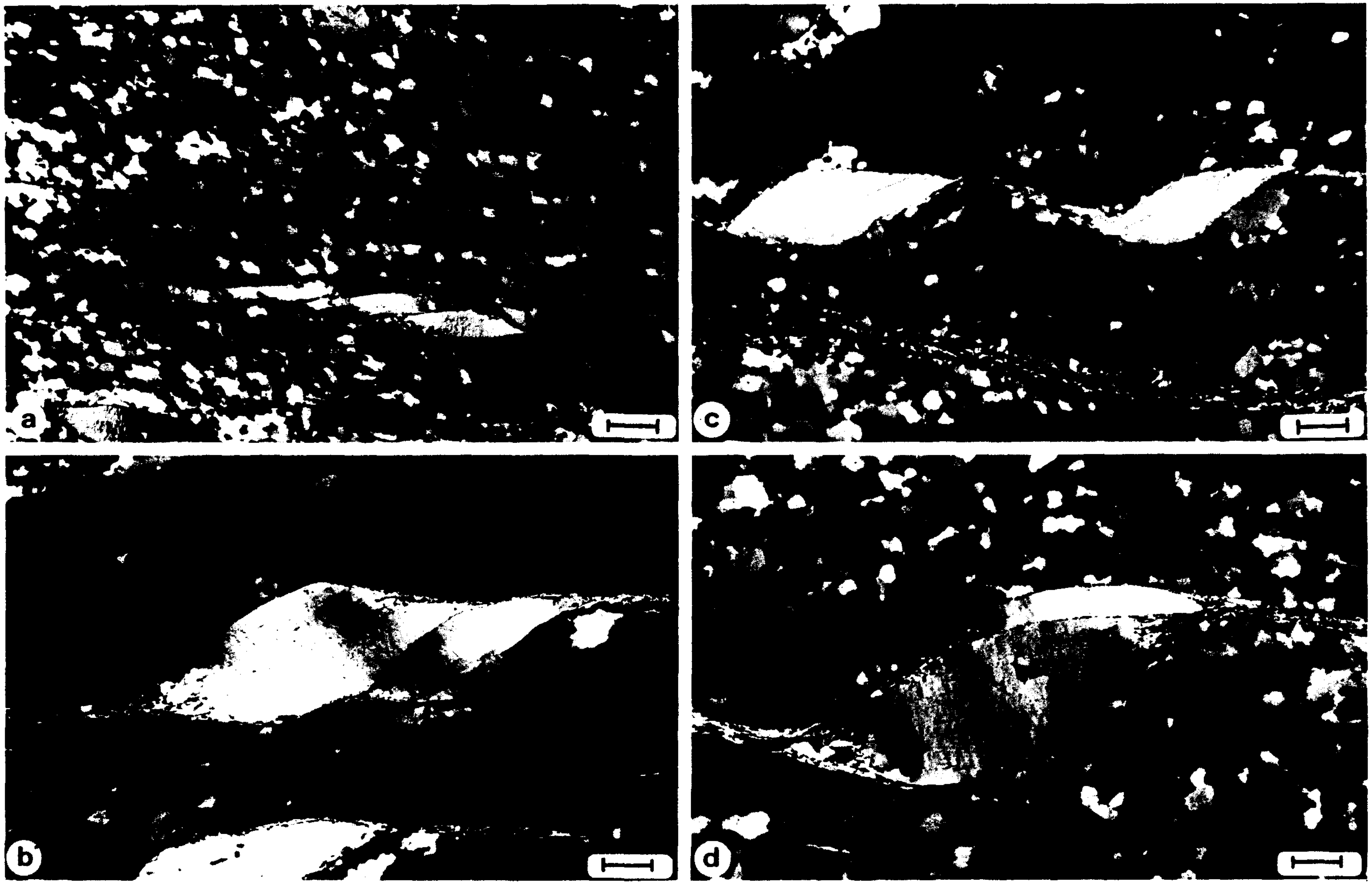

Fig. 7. Some of the mechanisms by which mica 'fish' multiply. Cleavage-split microfractures with (001) sub-parallel to the C-surfaces lead to new 'fish' in (a). In (b) with (001) inclined about 40° against the sense of shear, cleavage splitting leads to new 'fish' with the typical lenticular 'eye' form already developed (b). Relative movement on the cleavage fracture is antithetic to the bulk shear sense. In (c) a through-cleavage microshear generates a new 'fish'. The orientations of microshear bands so formed typically deviate in orientation from that of the bulk shear plane. In (d) a cleavage-split leads to 'over the top' generation of a new mica 'fish'. Example (a) comes from the Ruby Mountains, and (b, c, d) come from the Coyote Mountains, Arizona. Bulk sense of shear is sinistral in (a), dextral in (b, c, d). Scale bars are: (a) 100 μm; (b) 80 μm; (c) 150 μm; (d) 200 μm.

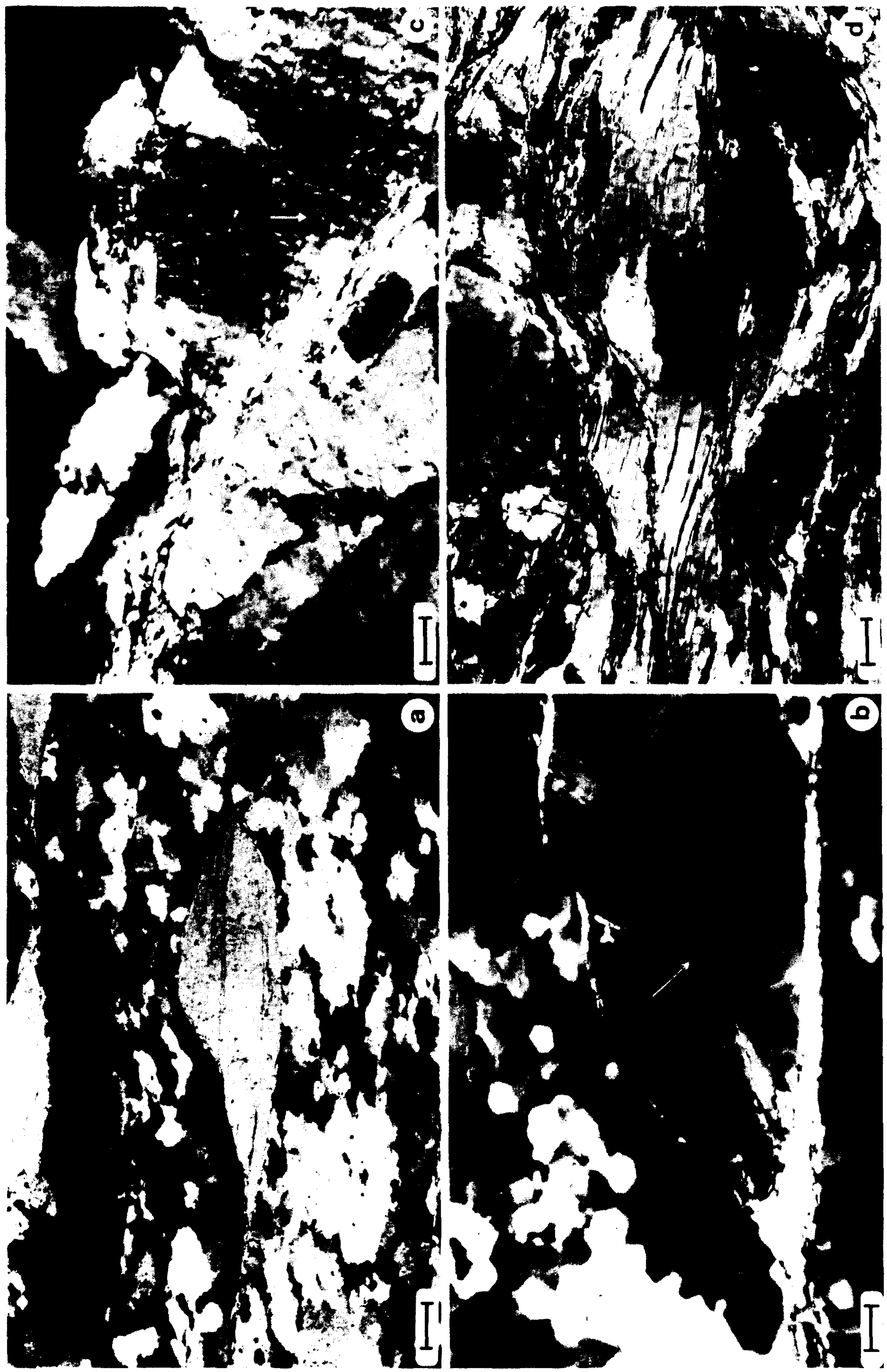

Fig. 8. A peculiar shape results when a 'fish' is peeled off the host clast as the result of the formation of microscopic 'listric normal' faults. This shape (a) has been found to be a reliable kinematic indicator. Sense of shear is sinistral in (a). Diagrams (b–c) show the process of formation of a new mica 'fish' arrested in its early stages. Arrows point to 'listric normal' microfaults. Diagram (d) shows a mica 'fish' transected by several discrete 'listric normal' microfaults. Bulk sense of shear is dextral in all cases illustrated. Relative movement on the 'listric normal' microfaults is generally antithetic to the bulk shear sense. Diagrams are from: (a) the Ruby Mountains, Nevada; (b) the Coyote Mountains, Arizona; (c) the Seve mylonite complex, Sweden; (d) the Betic Cordillera, Spain. Scale bars are: (a); 80 μm; (b) 40 μm; (c) 40 μm; (d) 80 μm.

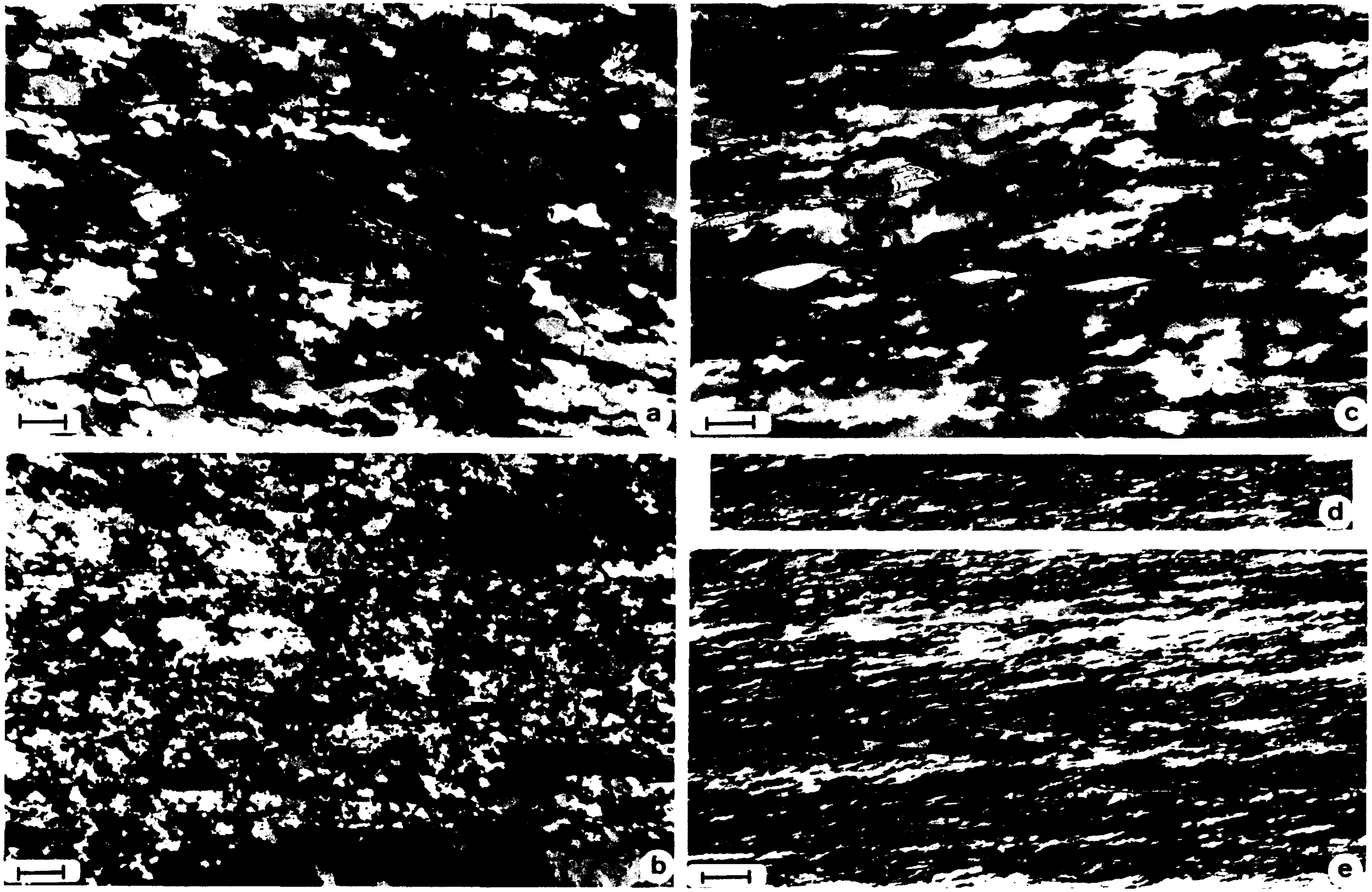

Fig. 9. Oblique foliations in dynamically recrystallized quartz aggregates, defined principally by elongate grain shapes, and grain-boundary alignments. The presence of sub-prismatic subgrain boundaries has little or no influence on the microstructure in (a). In (b) the microstructure is dominated by migration *recrystallization*, and *conjugate grain-boundary alignments* are developed. In (c) and (d–e) the microstructure is dominated by rotation recrystallization, and by grain-boundary alignments related to subgrain structure, and alignments of grains and subgrains with related orientations. In (d–e) alignments with different obliquities can be recognized on different scales (see text), and five different kinematic indicators can be recognized. Examples are from (a) the Coyote Mountains; (b) Naxos, Cyclades; and (c) and (d–e) from the Ruby Mountains. The shear sense is sinistral in (a) and (b), and dextral in (c) and (d). The scale bars are: (a) 80 μm; (b) 100 μm; (c) 100 μm; (d–e) 260 μm (same photo with different contrast).

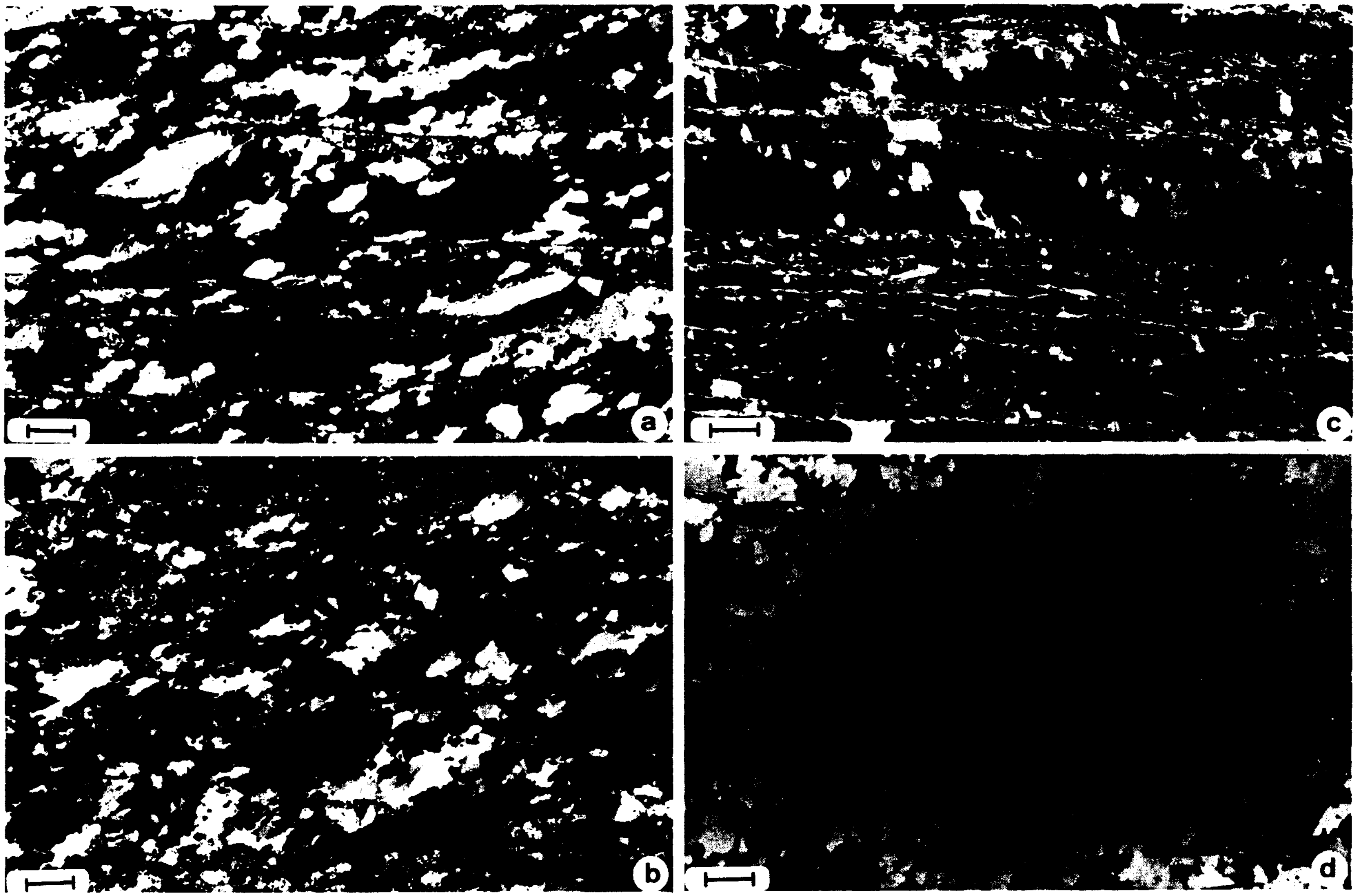

Fig. 10. Oblique foliations in dynamically recrystallized quartz aggregates. The foliation is defined by elongate grain shapes (a–b), trails of related orientations (a), grain-boundary alignments (a–d). The factors which control these alignments include the formation of 'prismatic' subgrain boundaries (c) and the interaction of migrating grain boundaries with these sub-boundaries. However, alignments are not necessarily affected by such factors (b). Recrystallization subsequent to deformation can wipe out oblique foliations in quartz, although the mica 'fish' can still be preserved (d). Diagrams are from the Coyote Mountains (a), the Ruby Mountains (b), the Platengneiss shear zone of the Austro-Alpine, Austria (c), and the Otztal mass, South Tirol (d). Scale bars are: 80 μm; (b) 100 μm; (c) 240 μm; (d) 260 μm.

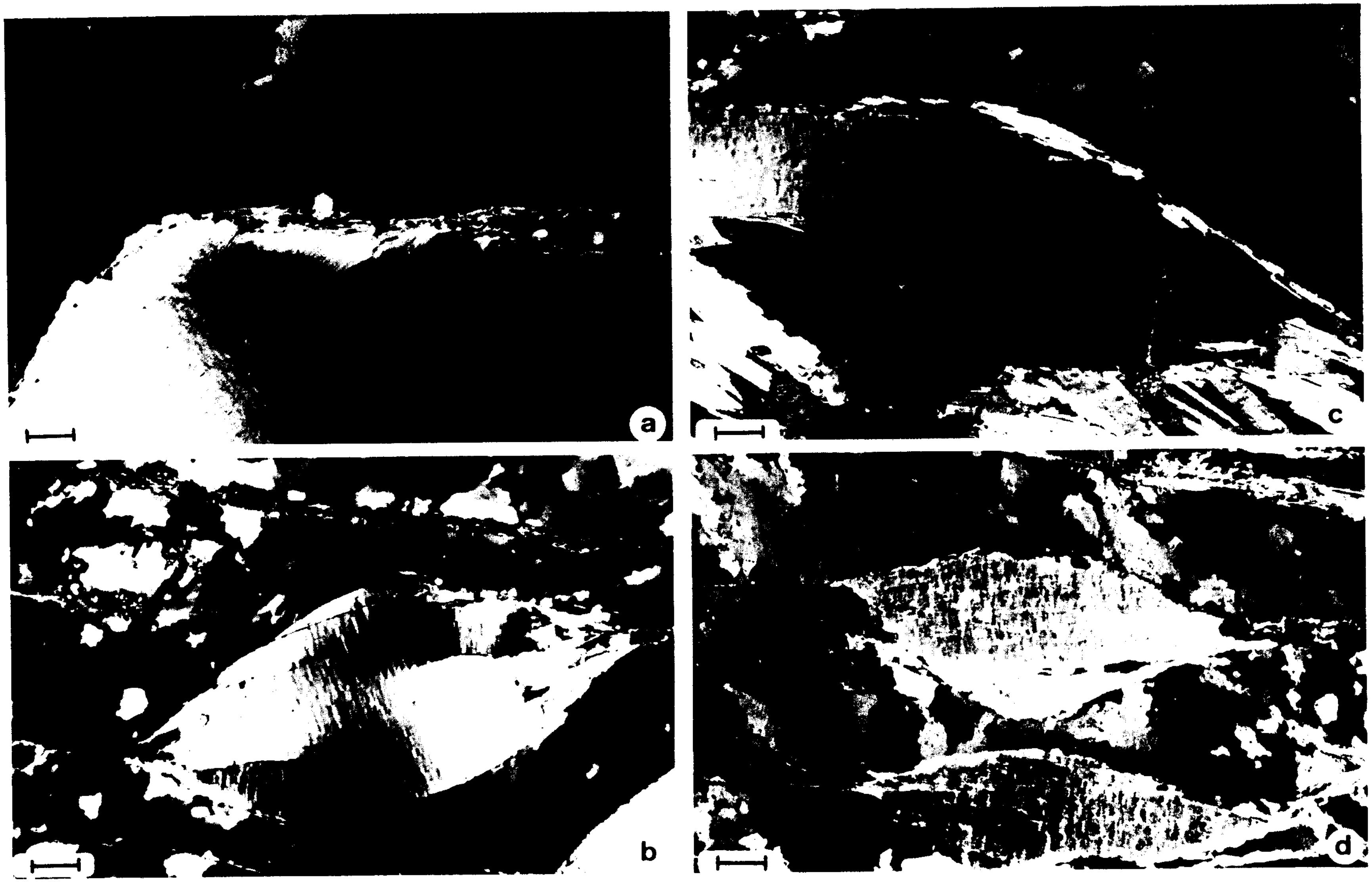

Fig. 17. Different effects of recrystallization on mica 'fish' and mica 'fish' trails. In (a) from the Coyote Mountains, the effect of differential shear at the boundary of a mica 'fish' is shown. The (001) cleavage is folded over parallel to the boundary, and distorted and disrupted. In (b) from the Ruby Mountains, internal recrystallization has led to asymmetric recrystallization fronts moving into the interior of the mica 'fish'. In (c) from a type I S–C tectonite (Windy point in the Catalina Mountains, Arizona), recrystallization has led to growth of new mica grains at the boundary of the 'fish', presumably from misoriented mica as shown in (a). In (d) from the Ruby Mountains recrystallization with significant grain boundary diffusion has led to a 'fish' whose outline has begun to change, and which has only one lattice orientation internally. Scale bars are: (a) 40 μm; (b) 80 μm; (c) 110 μm; (d) 80 μm.

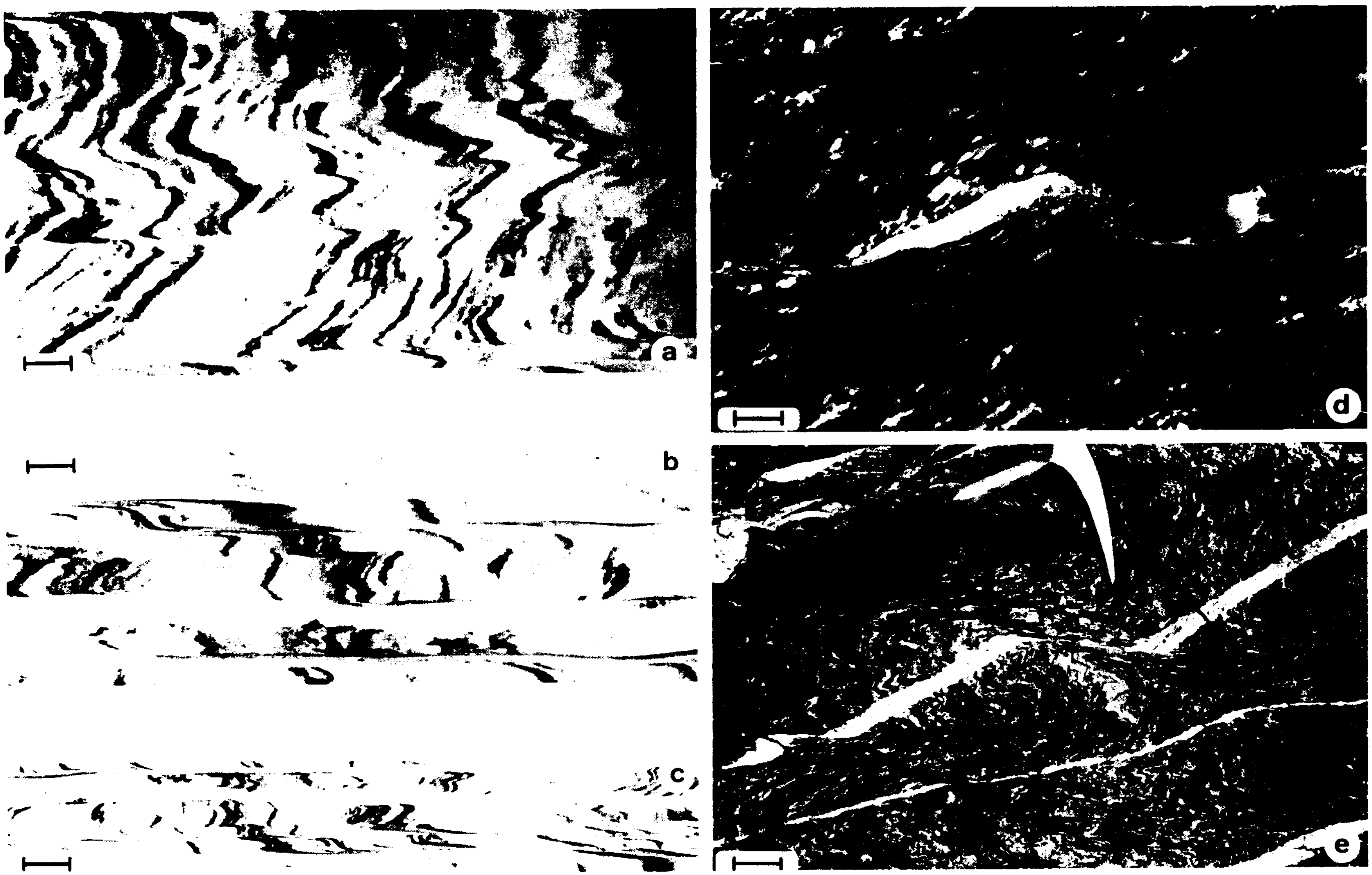

Fig. 18. Examples of S–C tectonites where complexities exist related to whether or not a pre-existing anisotropy is in the shortening field or the extension field of a later non-coaxial laminar flow. Diagrams (a–c) are from the marble quarry above Laas in the South Tirol, Eastern European Alps. Intense shear strains have been accommodated by very narrow shear bands in which shear strains between 100 and 2000 have accumulated. In (d) from the Ruby Mountains, a C-surface has been switched from the extension field to the shortening field. The result is that it folds, with the (oblique) grain elongation fabric in the adjacent quartz now in an axial plane relationship. In (e) from the Pinaleno Mountains the anisotropy was initially in the shortening field, and folding took place. At a later stage of the deformation, shear zones transected the body, and locally switched the anisotropy into the extension field. The aplite dyke which intruded axial plane to the folds indicates that a pulsation in the stress field took place before the shear zones formed. Scale bars are: (a) 3 cm; (b) 4 cm; (c) 8 cm; (d) 200 μm; (e) 4 cm.

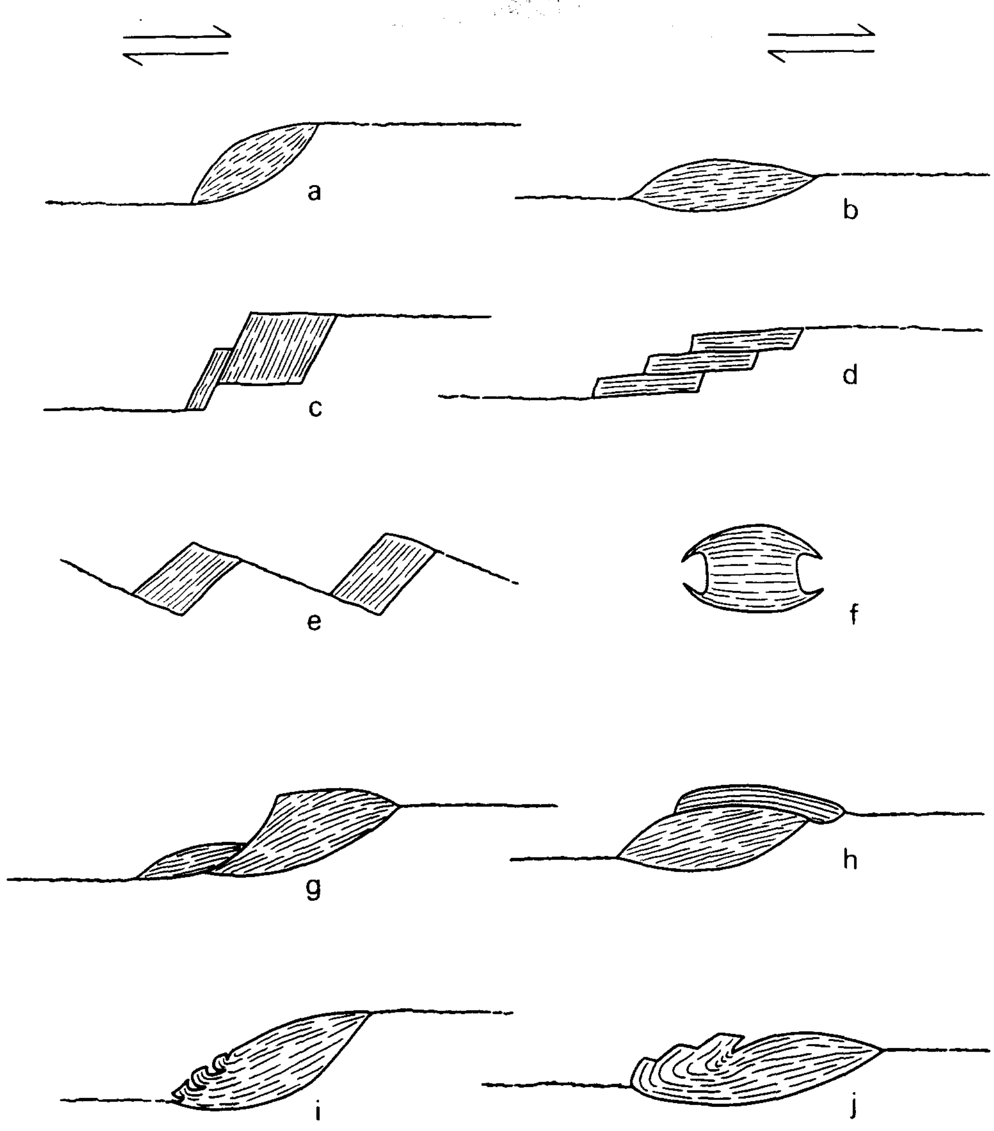

Fig. 5. The effect of variation in the attitude of (001) in mica 'fish' on microstructures, illustrating the mechanisms whereby mica 'fish' are peeled off their host clasts. Bulk sense of shear is dextral. New mica 'fish' are generated by fracture of a mica porphyroclast, involving combinations of cleavage fractures (c–d) or through-cleavage micro-faults (e). Mica 'fish' are usually tilted back against the sense of shear (dextral) but the angle of tilt varies from about 30° (a) to almost parallel to the C-surfaces (b). Cleavage-splits result in antithetic (c) or synthetic (d) microfaults. Through-cleavage microfaults are also common (e–f). Combinations of these two types of microfault lead to 'listric normal' microfaults (g) or 'thrust' microfaults (h), again depending on the orientation of the (001) cleavage. Even with the (001) plane tilted back 30° against the bulk flow plane, heterogeneities in the flow occasionally force the (001) plane into the shortening field, in which case on the rim of individual 'fish' tight to isoclinal folds can be found in the cleavage planes (i). When (001) is less steeply inclined, the entire 'fish' may be isoclinally folded (j).

A comment can be made on the deformation mechanism of muscovite in nature, since brittle processes are important in the production of 'fish' in this material. Fractures parallel the (001) cleavage are common, even though the mica is oriented with its easy slip plane in the ideal orientation for undergoing substantial shear. A model that explains this behaviour is that dislocation pile-ups at obstacles in the glide plane eventually result in the initiation of a cleavage fracture, suggesting that cross-slip and climb are difficult.

OBLIQUE FOLIATIONS IN DYNAMICALLY RECRYSTALLIZED QUARTZ AGGREGATES

The oblique foliations in the quartz aggregates adjacent to the mica 'fish' trails (Figs. 9 and 10) are defined by combinations of the following elements: (a) elongate grain shapes (these can include ribbon grains as well as recrystallized grains with smaller aspect ratios); (b) alignments of segments of the traces of the enveloping surfaces to grain boundaries or groups of grain boundaries; (c) elongate zones in which the crystallographic orientations of the recrystallized grains appear to be related. These alignments of families of related orientations are best seen with the gypsum (i.e. first order retardation) plate inserted. These microstructures are related to the effects of dynamic recrystallization of the quartz.

If it were possible to examine the quartz aggregates between the mica 'fish' trails as they recrystallized, one might expect to see individual grains slowly elongating,

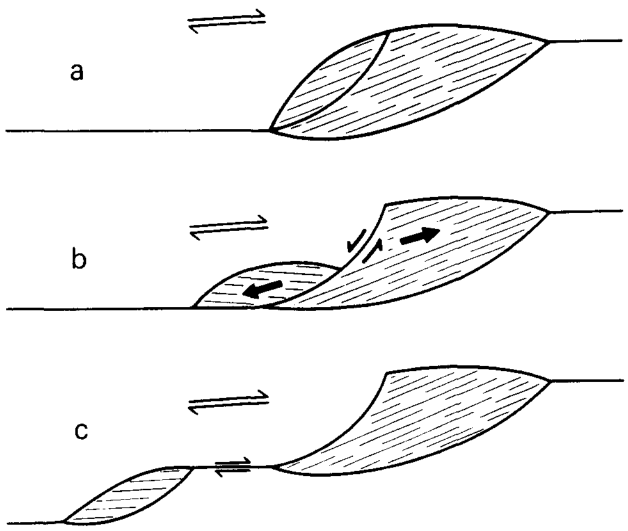

Fig. 6. A peculiarly shaped mica 'fish' develops because of the following sequence. First a listric normal fault forms, antithetic to the bulk shear sense (a). The newly formed mica 'fish' is then pulled apart from its host clast, because the (001) plane lies in the extension field of the bulk deformation (b). The (001) planes misorient as this occurs, since the boundary fault is curved. Finally the newly formed 'fish' and its host clast are separated by a synthetic displacement discontinuity (c). Mica 'fish' with this shape have proved to be reliable kinematic indicators.

so that with increasing strain they rotate towards parallelism with the C-surfaces (Fig. 11). However, when recrystallization takes place, the finite-strain 'clock' is effectively reset, so that in a newly recrystallized volume the process of elongation and realignment is restarted. If the oblique foliation is related to grain shape, this recrystallization process results in different degrees of obliquity in different parts of the thin section. The attitude of the oblique foliation will depend on the shear strain accumulated since the particular volume of rock last recrystallized. Alignments closest to the C-surfaces are the alignments related to the oldest cycle of recrystallization. The fact that 2 or 3 different alignments can be recognized in some mylonites suggests cycles of recrystallization as flow progressed. In these circumstances, the oblique foliation can be aligned anywhere between 10 and 40° away from the C-surfaces.

Law *et al.* (1984) have recognized oblique foliations such as those described here, in the Moine mylonites in Scotland, and suggest they are examples of steady-state foliations, as discussed by Means (1981). Such steady-state foliations will result when continuous dynamic recrystallization leads to constant resetting of the 'finite-strain clock' and hence to statistical constancy of the attitudes of the alignments that define the oblique foliation.

In circumstances dominated by rotation recrystallization (Poirier & Nicholas 1975, Poirier & Guillopé 1978) progressive misorientation leads to the development of high-angle grain boundaries, which undergo only limited migration. Progressive recrystallization under these circumstances may lead to progressive reduction in grainsize, as smaller and smaller subgrains reach critical misorientations, until a stable grainsize is reached determined by the rate of grain growth. For example, glide polygonization may first lead to the development of kink-like substructures, and progressive misorientation of these subgrains then leads to the formation of ribbon-grains. Continuing deformation may increase the misorientation across subgrain walls internally in each ribbon grain, until finally rotation recrystallization takes place. The result is that different alignments can be recognized on different scales in the thin-section, because pre-existing grain outlines are still evident, in spite of subsequent 'internal' recrystallization (Fig. 11).

Figure 9(e) shows ribbon grains that have recrystallized internally illustrating this effect. In this particular example (Figs. 9d & e) there are five independent kinematic indicators: (a) asymmetric mica 'fish'; (b) stair-stepped mica 'fish' trails; (c) ribbon grains inclined at about 10–20° to the C-surfaces; (d) recrystallized ribbon grains, defining a second alignment inclined at about 20° to the attitude of the ribbon grains and (e) asymmetric quartz *c*-axis fabrics (discussed in a later section). Each indicator gives the same answer for the sense of shear.

In circumstances dominated by migration recrystallization (Poirier & Guillopé 1978) different microstructures develop, depending on the interaction of migrating grain boundaries with other elements in the microstructure (e.g. Figs. 9b, 10b & c). The shape of the recrystallized grains can never become too elongate if grain boundaries continuously migrate, or if the microstructure is continuously affected by new waves of recrystallization (Fig. 12). Different microstructures are to be expected depending on the rate of grain boundary migration relative to the imposed strain rate. If crystal plastic processes dominate, alignments defined by grain elongations will be closer to the bulk flow plane than in the case when grain-boundary migration is relatively rapid. In the latter case, grainsizes will be larger, the degree of elongation will be lower, and the attitude of the S-surfaces will be further away from the bulk plane, for example 40° away from the C-surfaces.

If the orientation of oblique foliations is controlled principally by grain elongation, then the attitude of the oblique foliation might be expected to be approximately that of the XY plane of the local finite-strain ellipsoid (time zero set at the time the volume last recrystallized). In this case, for simple shear, the existence of the oblique foliation would not be recognized until it is within *ca* 40° of the bulk flow plane, and alignments at larger angles to the C-surfaces should not form. However, grain-boundary alignments at angles of up to 70–80° to the C-surfaces are occasionally observed (Fig. 10c), therefore additional controls on the orientation of grain-boundary alignments must exist (Figs. 13 and 14).

Interaction of migrating grain boundaries with subgrain structure may give rise to alignments of grain boundaries at high angles to the C-surfaces. Migrating grain boundaries may slow down when they encounter a significant misorientation in the host, e.g. an optically visible 'subgrain' boundary (Fig. 13b, see Urai 1983). Sub-

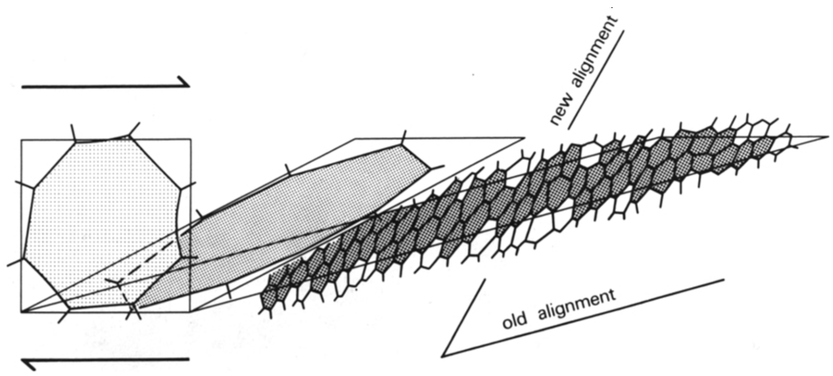

Fig. 11. Dynamic recrystallization periodically resets the 'finite-strain clock'. Diagrams show a sequence where a grain deforms and then internally recrystallizes (by a combination of rotation and migration recrystallization), and the new recrystallized grains in turn become elongate as deformation goes on, defining a new oblique foliation. The elongate shape of the 'old' grains can still be recognized by virtue of a clustering of the orientations (stippled) of the new grains.

prismatic subgrain boundaries in quartz are common, and these commonly have preferred alignments at high angles to the extension lineation, simply because plastically deformed quartz aggregates usually exhibit patterns of preferred crystallographic orientation with a single ⟨**a**⟩ direction aligned close to the bulk shear direction. If recrystallization takes place so that subgrain structure affects grain-boundary alignment, then oblique foliations form at high angles to the extension

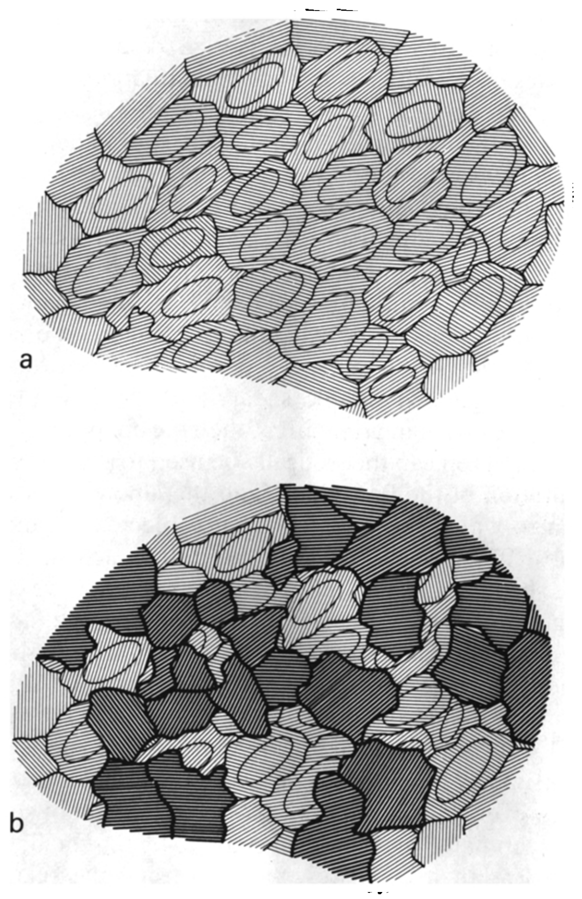

Fig. 12. Dynamic recrystallization resets the 'finite-strain clock' in another way when migration recrystallization takes place. In diagram (a) grains have become elongate and a weak grain-boundary aligment is observed. However, before grains can be too elongate, they are consumed as the result of grain boundaries sweeping across the microstructure. The 'finite-grain clock' is thereby effectively reset. The newly grown grains are shown darker.

lineation (e.g. Fig. 10c). There are numerous cases, however, where the alignment of grain boundaries is at 20–40° to the dominant subgrain-boundary orientation, so only in specific circumstances does preferred alignment of subgrain boundaries control the orientation of aligned grain boundaries in deformed and recrystallized quartzite.

Some oblique foliations are controlled by grain-boundary alignments (e.g. Figs. 9b and 14a), usually in circumstances where migration recrystallization dominated the microstructure. These alignments have been suggested by Lister & Dornsiepen (1980) to be the result of interaction between rapidly migrating grain boundaries with microscopic shears or slides initiating at suitably oriented grain boundaries (Fig. 14b). These slides or microshears may exert mimetic control on the attitude of the migrating grain boundary as the result of segregation of impurities, or second phase particles. Small second phase 'impurities' on the C-surfaces pin the migrating grain boundary and hinder the movement of boundaries attempting to cross the C-surfaces (Fig. 14c). A similar effect may be involved when slip polygonization leads to the development of kink-like structures which evolve into ribbon grains. Growth of small second-phase 'impurities' on the new formed grain boundaries hinders their further migration, and is an important factor leading to the development of oblique foliations.

QUARTZ *C*-AXIS FABRICS

Questions concerning the asymmetry of quartz *c*-axis fabrics in shear zones have been discussed extensively in the literature, and the reader is referred to five recent papers, namely those by Bouchez & Pecher (1981), Bouchez *et al.* (1983), Lister & Williams (1979), Behrmann & Platt (1982) and Simpson & Schmid (1983). Of interest to us here are two methods for determining the sense of shear using quartz *c*-axis fabrics: (a) skeletal analysis, a technique proposed by Lister & Williams (1979) and applied by Behrmann & Platt (1982); and (b) various techniques concerned with asymmetry of the *c*-axis or *a*-axis orientation distribution (see reviews by Bouchez *et al.* 1983, Simpson & Schmid 1983).

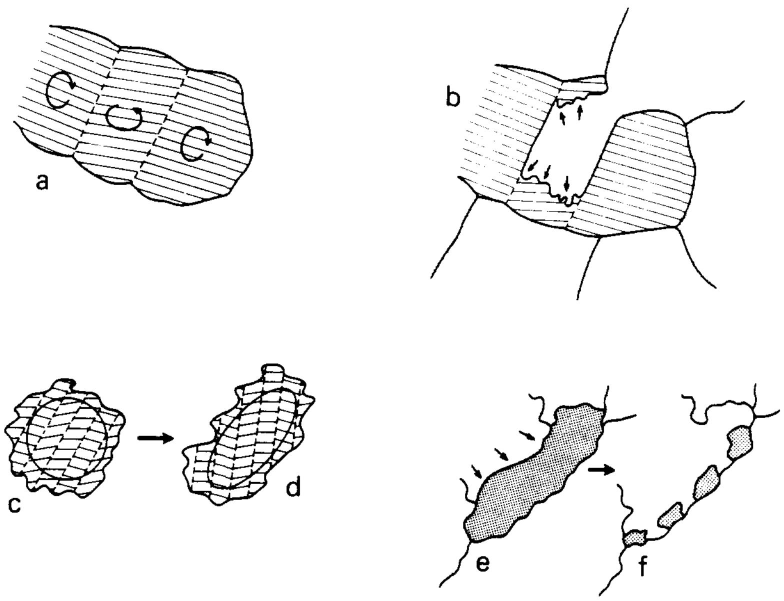

Fig. 13. Factors that affect the development of oblique foliations in dynamically recrystallized quartzite are illustrated. Glide polygonization leads to the formation of kink-like structures (a). Grain-boundary migration is sensitive to the relative orientation of the lattic of the grain being consumed ahead of the migrating recrystallization front. Migrating grain boundaries may stop or slow down in the vicinity of subgrain boundaries (b). Grain elongation can also lead to a statistical alignment of grain boundaries (c–d). Such alignments of families of grains with related orientations can also help mark oblique foliations, and one mechanism for producing such alignments is shown in (e–f).

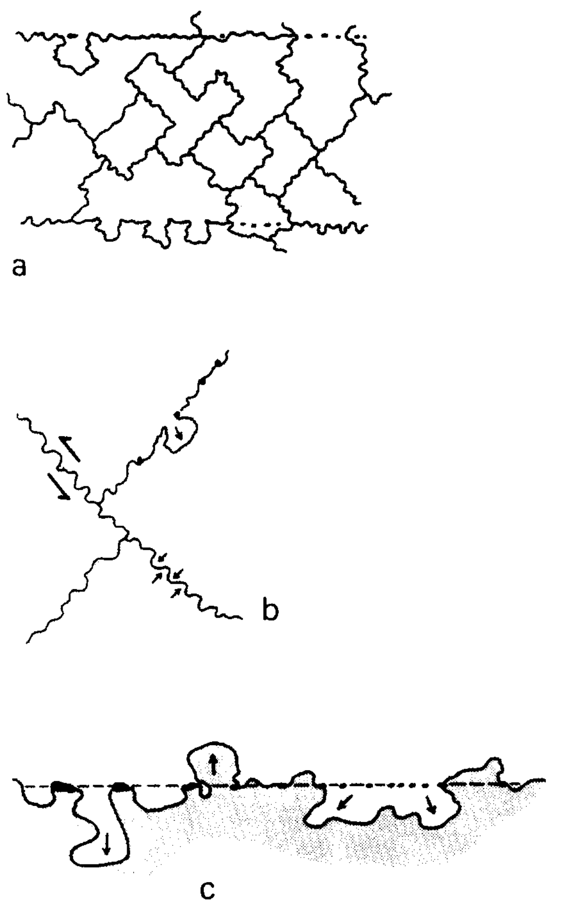

Fig. 14. Grain boundary alignments at higher metamorphic grades can be caused by the interaction of migration recrystallization with grain boundary slides and microshears. Strong (conjugate) grain boundary alignments (a) result if boundaries sweep up to the position of the microshear and then decelerate. Microstructures such as (b) are diagnostic for the prior existence of a grain boundary microshear. Trails of small second phase grains (for example on C-surfaces) also lead to grain-boundary alignments (c) as a result of effects related to the pinning of migrating grain boundaries.

Behrmann & Platt (1982) and Garcia Celma (1982, 1983) demonstrate effects related to domainal variation of fabric, and Behrmann & Platt (1982) demonstrate the advantages of skeletal analysis in this situation.

Quartz *c*-axis fabrics have been measured in a number of the S–C mylonites illustrated in this paper. The asymmetry of the fabric with respect to the C-surfaces gives a clear indication of the sense of shear, and this is consistent with the sense of shear obtained using the other kinematic indicators which have been so far described. This work allows a comment to be made on one puzzling fact to do with the asymmetry of quartz *c*-axis fabrics in highly sheared rock. If fabrics form during progressive simple shear, and the flow plane remains constant in orientation, then the obliquity of the fabric skeleton can theoretically be used to estimate the orientation of the flow plane, and the amount of shear strain to which the rock has been subjected (Lister & Hobbs 1979, Bouchez *et al.* 1983). In this case, for very large shear strains, the fabric skeleton should have only a slight obliquity to the C-surfaces, assuming the C-surfaces have an orientation close to that of the bulk shear plane. Typical quartz *c*-axis fabrics from the Coyote Mountains, and from the Ruby Mountains, are shown in Fig. 15, and since these fabrics have these characteristics, some support is gained for these assertions.

However, in a number of cases, the amount of shear strain estimated in this way appears to be too small, and much less than estimates obtained using the relative displacements between mica 'fish' as a guide. This is probably because the fabric skeleton is sensitive to changes in the movement picture during the closing stages of deformation. If folds begin to develop, the instantaneous stretching axes rotate away from their initial orientation; and even if only 20% additional strain

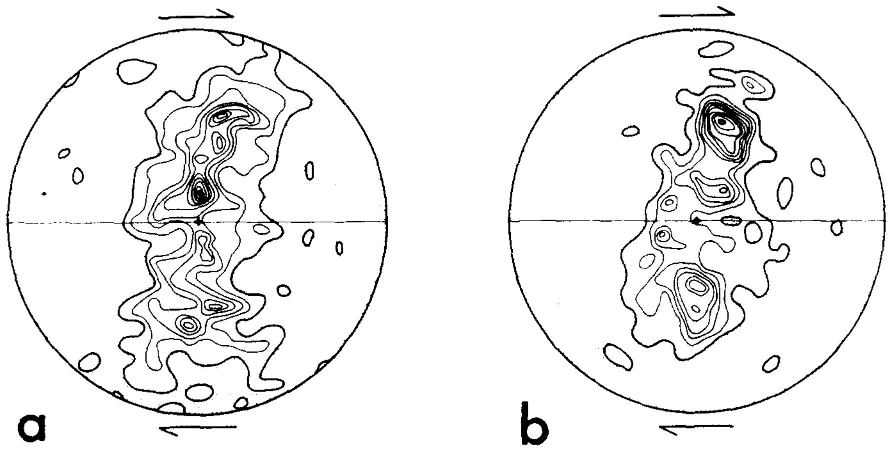

Fig. 15. Typical c-axis fabrics in type II S–C mylonites from the Coyote Mountains and the Ruby Mountains metamorphic core complexes. Girdles are only slightly inclined to the C-surfaces, consistent with the large shear strains undergone. In (a) from the Ruby Mountains (R15) 250 grains were measured, and in (b) from the Coyote Mountains 312 grains were measured. Sense of shear in both cases is dextral.

is involved, and a finite structure is hardly discernible, the fabric skeleton can be rotated 10° away from its original position. This type of effect commonly takes place in mylonite zones in localities where folds have developed, for example in the Ruby Mountains (see figs. 12 and 15b of Snoke 1980), and in the mylonites of the Cap de Creus (Carreras *et al.* 1977). It is fortunate that these changes usually occur in such a way that they accentuate the obliquity of the fabric skeleton, and do not reverse it.

THE EFFECTS OF RECRYSTALLIZATION ON MICA 'FISH'

Trails of mica 'fish' are easy to recognize if the original microstructures are preserved. However, in some cases, although a rock mass may have experienced intense non-coaxial laminar flow during an earlier stage of the deformation history, subsequent events have obliterated microstructural evidence for the non-coaxial character of the initial deformation. Recrystallization is particularly notorious in this regard. It is, therefore, not surprizing that evidence of large-scale non-coaxial flow usually comes from rocks which have experienced deformation while mean stress and temperature both decreased. If mean stress and temperature are increasing during deformation, and intense non-coaxial laminar flow takes place, subsequent deformation events and associated recrystallization ensure that most of the kinematic information about the early history is difficult, or impossible, to discern.

In rocks subject to complex histories, there would seem little chance for the preservation of oblique foliations in the dynamically recrystallized quartz aggregates, since microstructures in quartz are particularly susceptible to modification by later events. Figure 10(d) shows what is most likely a Hercynian mylonite subjected to Alpine reheating (from the Otztal massif, South Tirol). No evidence of mylonitization remains in the (recrystallized) quartz microstructure. Mica 'fish', however, are less easily modified, and remain as the only indicator that early deformation may have involved (intense) non-coaxial laminar flow.

In the following two sections, the effect of recrystallization on mica 'fish' will be described, pointing out the different circumstances that result depending on whether or not significant grain-boundary diffusion accompanies grain-boundary migration.

Recrystallization without diffusion along the grain boundaries

The moving grain boundary may simply involve transfer of groups of atoms and ions across the interface. The process does not necessarily involve diffusional mass-transfer along the migrating grain boundary. As the grain boundary sweeps across the structure, material simply changes its crystallographic orientation, not its spatial location. Movement of the recrystallization front involves no metamorphic transformations or changes of composition of any kind.

A necessary corollary of this type of behaviour to the exclusion of all other types of recrystallization, is that only grain boundaries separating the same mineral species are mobile. In other words a mica 'fish' surrounded by quartz may be capable of recrystallizing internally, but is not capable of any change in its external shape or form.

Microstructures which suggest this type of recrystallization are illustrated in Figs. 16 and 17. Shear at the boundaries of a mica 'fish' rotates the cleavage plane towards parallelism with the boundary. These are the most likely sites for the initiation of recrystallization, since as shown in Fig. 17(a), differential shear bends the distorted and disrupted (001) segments until they become parallel to the boundary of the 'fish'. Migration recrystallization involving rapid growth parallel to directions lying in the (001) plane initially results in asymmetric microstructures as illustrated in Fig. 16(a). The recrystallization front then begins to penetrate into the

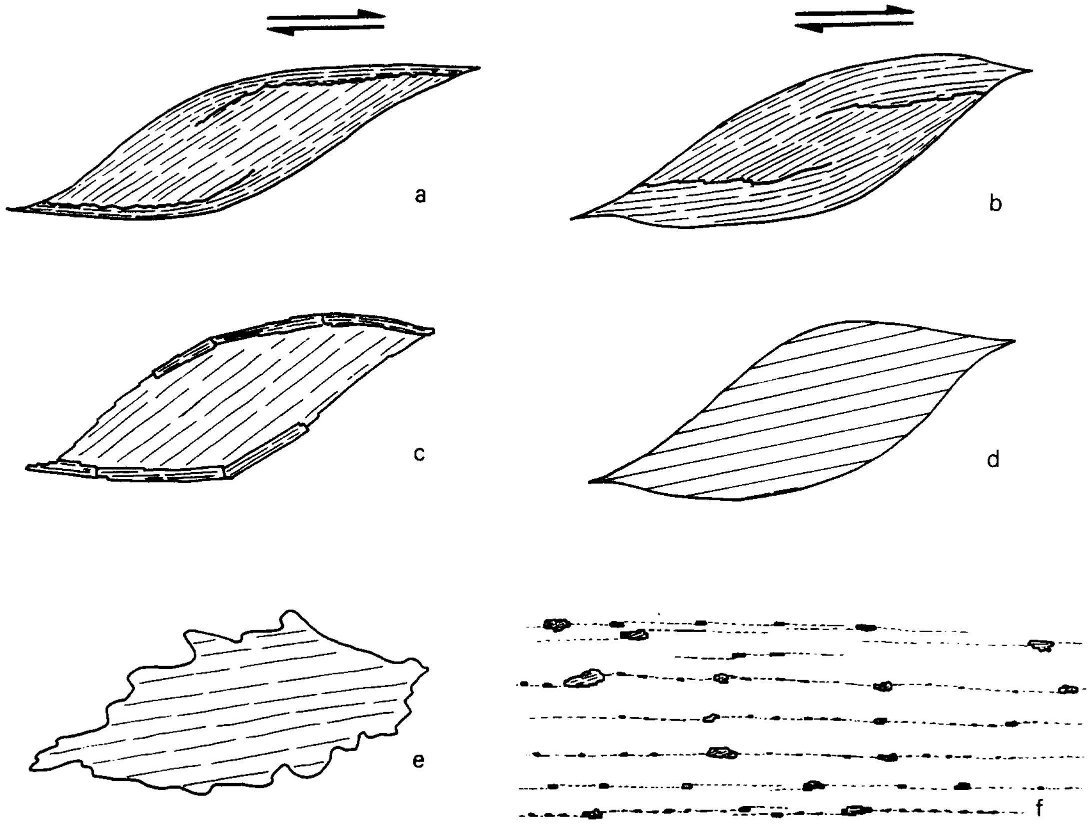

Fig. 16. The (001) cleavage at the edge of a mica 'fish' is often sheared over parallel to the boundary, and new growth initially results in the microstructure shown in (a). Continued recrystallization results in the thin skin of new grown mica expanding into the interior of the mica 'fish' (b). The recrystallization front is approximately parallel to (001). Occasionally, however, new mica grains form on the exterior part of the 'fish' (c). At higher grades one lattice orientation can take over the entire mica volume (d). With significant grain-boundary diffusion, the external shape or form of the mica 'fish' can change (e), and the microstructure defined by mica 'fish' and trails linking the 'fish' is strongly modified (f).

interior of the clast, migrating in a direction roughly perpendicular to (001). Microstructures as in Figs. 16(b) and 17(b) result.

Migration of recrystallization fronts, without significant mass-transfer by diffusion along the migrating grain boundaries, can eventually result in replacement of the deformed mica clast by only one lattice orientation, without disturbance of external shape or form (Fig. 16d) of the clast. Since mica 'fish' do not generally form from a single crystal host without bending and distorting the cleavage planes, the existence of mica 'fish' with an almost undistorted lattice suggests this type of recrystallization has taken place.

Recrystallization with significant diffusion along grain boundaries

Under conditions favouring diffusion, such as high temperature, significant mass transfer may take place along the grain boundary at the same time as it migrates. This means that grain boundaries separating two phases may also be mobile, and grain boundary diffusion will then allow mica 'fish' to change their external shape and form (Figs. 16e and 17d).

Trails of small blocky white micas (Fig. 16f) are common in medium grade deformed metamorphic rocks, and commonly these trails link larger (also blocky) mica grains. The grain boundaries of these micas can be quite irregular (Fig. 16d), and the trails usually separate quartz-rich areas in which extensive migration recrystallization took place. The presence of the mica trails seems to have hindered migration of grain boundaries attempting to cross from one quartz-rich domain to another; for example as observed in upper-amphibolite facies 'ribbon mylonites'. Such microstructures may indicate relict C-surfaces in which the mica has undergone extensive recrystallization, so that the characteristic 'fish' shape is not preserved. Since such microstructures are commonly encountered in medium grade metamorphic rocks, by implication major zones of non-coaxial laminar flow may be more prevalent than is currently acknowledged. The microstructural evidence for the existence of such zones is all too easily removed by subsequent recrystallization.

A BROAD CLASS OF S–C TECTONITES

Because of the importance of S–C relationships as kinematic indicators, we suggest the creation of a broad class of S–C tectonites. This concept of an S–C tectonite is something quite distinct from the classical tradition of purely geometric analysis of foliation and time relationships. The nature of the macroscopic structure is passed over in favour of determining the kinematic significance of the various structural elements.

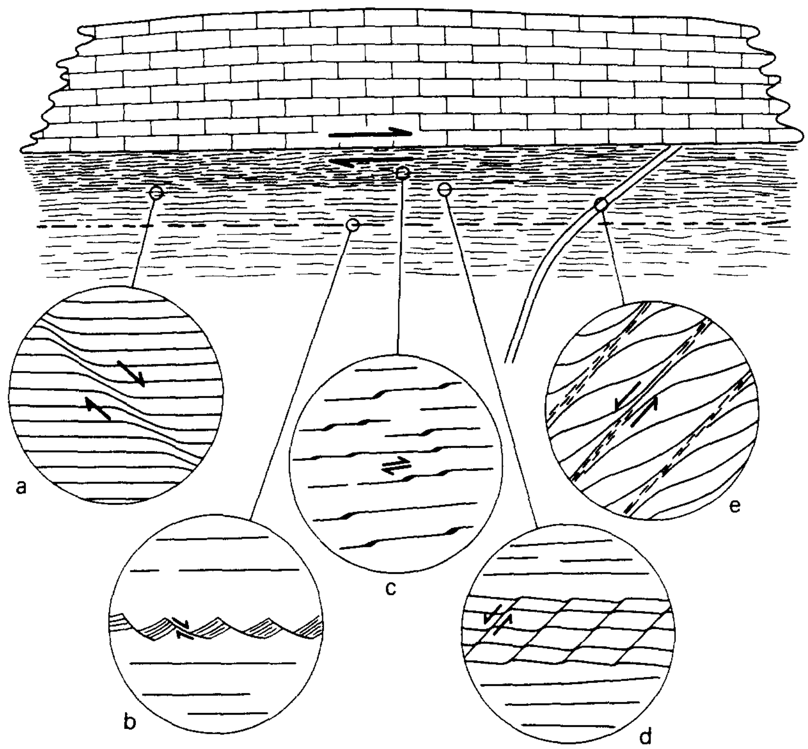

Fig. 19. Complexities in S–C relations beneath a (subsequently rotated) low-angle normal fault. The non-metamorphic upper plate is underlain by S–C mylonites. Low-strain shear bands have formed with orientations strongly divergent from that of the bulk shear plane, presumably as a response of the anisotropy to stretching (a). These shear bands may be synthetic or antithetic to the bulk shear sense. Individual layers may be asymmetrically sliced by these shear bands (b), with foliation being back-rotated by spin countering the effects of asymmetrical shear. Fortunately, type II S–C mylonites also occur (c), and since these record very high shear strains, they are a reliable indicator of both the orientation of the bulk shear plane, and the bulk (dextral) shear sense. Antithetic shears are common in individual bands (d), and in suitably oriented heterogeneities. The cross-cutting dyke (e) is spun clockwise and layer-parallel shear results in antithetic shear sense in the deformed dyke rock.

The usage of the term S–C tectonite can be extended to cover any deformed rock in which there are two families of surfaces, S-surfaces and C-surfaces. The term S-surface can be used as a general term for a statistically defined foliation in the sense of Paterson & Weiss (1961). Alternatively, S-surfaces may be regarded as primarily the result of the accumulation of finite strain, and usage of the term S-surface restricted to foliations which are approximately parallel to the local orientation of the *XY* plane of the finite strain ellipsoid. The term C-surface can be used to describe the orientation of displacement discontinuities developed during flow, as well as being applied to describe the locus of zones of relatively intense shear strain.

However, it is often difficult to interpret the significance of S–C relationships without some understanding of the macroscopic structure, since the movement picture can vary in a complicated way from place to place, for example as illustrated in Figs. 18 and 19. If shear bands involve only low shear strains, they can deviate significantly in orientation from the attitude of the bulk shear plane (Fig. 19). In this case both synthetic and antithetic relationships are common, and obviously it is difficult to use such microstructures to infer the orientation of the bulk shear plane, or even the bulk shear sense, without a fairly detailed understanding of the macroscopic structure. Such problems are not encountered when S–C relationships have been formed by deformations involving large shear strains (Fig. 19c).

Recognition of S–C relationships involving large shear strains allows the statement that (on the scale of observation) intense non-coaxial laminar flow has taken place, and locally the orientation of the bulk shear plane and direction of shear can be estimated. The sense of shear is immediately apparent.

Examples of S–C tectonites are numerous, falling into three categories depending on the timing relationships between the S- and the C-surfaces.

S–C Tectonites where both surfaces form in the same deformation

We have already discussed the case when S- and C-surfaces form synchronously, or during the same deformation. It is probably more common that the mylonitic foliation forms early in the deformation history, and the C-surfaces begin to form later as a response to the development of anisotropy. The C-surfaces are then merely the later stages of the evolutionary process by which foliations form (see also Platt & Vissers 1980).

S–C Tectonites where an S_1–S_2 *terminology is justified*

The case when C-surfaces form during the last stages of the deformation which produced the S-surfaces may fall under this category, but the situation we have in mind is that of an older metamorphic complex involved in a later shear zone, where older S-surfaces are trans-

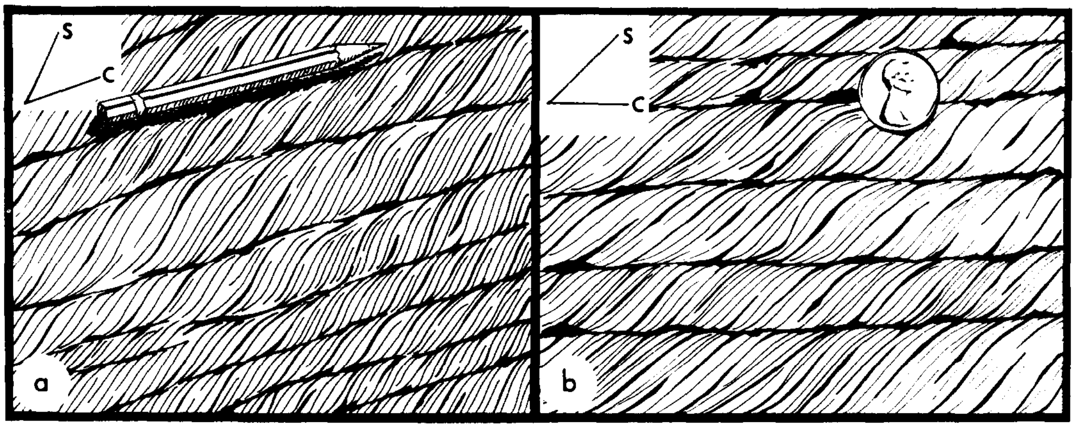

Fig. 20. Button schists of the SE Appalachian Piedmont. An example of S–C relations developed in metapelitic schists. Modoc zone, South Carolina Piedmont, southern Appalachians.

ected by C-surfaces produced during the younger deformation.

The most important factor which determines how structures will develop under these circumstances is whether the older anisotropy finds itself in the extension field or the shortening field of the later flow. If the pre-existing anisotropy is in the extension field, foliation boudinage will take place or extensional crenulations will develop as the result of the development of shear bands (Platt & Vissers 1980). In many S–C tectonites, the dominant foliation is in fact an older modified fabric, a circumstance which can be misleading in terms of the qualitative assessment of strain during mylonitization.

Platt & Vissers (1980) suggest that extensional crenulation cleavages can form during progressive deformation, successive sets of shear bands forming as older sets of shear bands rotate into the main fabric. In this case the older fabric is intensively modified, and S_1–S_2 terminology is not justified. However, in other circumstances the pre-existing foliation may be merely stretched, and rotated towards the bulk shear plane, at the same time being transected by (discrete) shear bands. This appears to be the case in the 'button schists' of the Southern Appalachian Piedmont (Fig. 20). In the mylonitic rocks from the Ruby Mountains, the obvious mesoscopic foliation is commonly related to C-surfaces which transect micaceous layers formed as differentiated axial plane schistosity in a previous (unrelated) part of the deformation history.

The case when the pre-existing anisotropy is in the shortening field of the later flow is illustrated in Fig. 18. The pre-existing anisotropy usually folds rather than accommodating the imposed shortening by uniform flow. The spectacular examples illustrated in Figs. 18(a)–(c) are from a marble quarry behind Laas in the South Tirol, Eastern European Alps. The rock is cut by narrow (0.1–10 mm wide) shear zones in which the pre-existing layering has been rotated into the extension field. Note the enormous shear strains which accumulated in these narrow zones (even assuming up to 100% extension of the material in between the zones, shear strains between 100 and 2000 have taken place).

Figure 18(e) illustrates a more complicated situation, in an example from the Pinaleno Mountains, Arizona, a metamorphic core complex described by Thorman (1981). In early stages of the deformation, the anisotropy was folded. In later stages, it was transected by shear zones. It can be seen that the stage of folding was separated from the stage at which localized shear zones began to form, since aplite veins have been intruded parallel to the axial plane of the folds, and then sheared. This relationship has some unusual implications concerning the local stress history, but field relations suggest that an ongoing deformation process was involved (Thorman 1981).

S–C Tectonites where there are folded C-surfaces

During ongoing deformation, changes in the pattern of flow can switch earlier formed C-surfaces into the shortening field. Only a few degrees rotation of the bulk flow plane is necessary. The result can be as illustrated in Fig. 18(d) which shows a folded mica 'fish' trail, where the synchronously developing oblique foliation in the adjacent dynamically recrystallizing quartzite has now an axial plane relationship. The relationships can be more complex, for example if previously formed C-surfaces are folded during a later deformation, and axial plane S-surfaces form that have no relationship whatsoever to the previous mylonitic history. In this case the C-surfaces can be termed S_1, and the later formed S-surfaces S_2.

When large shear strains are involved on individual C-surfaces, they usually have orientations close to the local orientation of the flow plane, and they therefore readily pass into the shortening field during the same deformation in which they formed, for example as the result of a local perturbation of the local flow field. The result will be that the C-surface is contorted and folded by ongoing deformation, with S-surfaces related to accumulating finite strain continuing to develop, but now in an axial-plane relationship to the folding C-surface (Fig. 18d). This type of effect can occur on a larger scale, for example when a rock slice (either a 'thrust slice' or an 'extensional allochthon') is caught up in a zone of laminar flow. The slice may be initially stretched so that mylonites develop, but then a variation in the flow field sets the slice into the shortening field, at which stage it contorts and begins to fold internally as well as externally.

The situation seems to apply to the Ruby Mountains where one of the uppermost slices (an extensional allochthon) is folded during a late stage of the mylonitization event. In this slice, *c*-axis fabrics are commonly inclined more than 20–30° to the C-surfaces. Although the inclination of the *c*-axis fabrics may give the correct sense of shear, caution needs to be exercised since it is clear that the asymmetry in this case is related to effects to be expected in a flow involving spin. Obviously, especially in cases such as these, it should not always be assumed that C-surfaces are within a few degrees of the bulk flow plane, even if they appear to have been associated with the accommodation of large shear strains.

RHEOLOGICAL IMPLICATIONS OF THE EXISTENCE OF SHEAR BANDS

The existence of shear bands has rheological implications in either, or both, of the following directions: (a) because shear bands commonly seem to develop after a foliation has developed, shear bands may be the result of a local yield phenomenon, for example, involving a critical yield stress; (b) because shear bands lead to intense shear strains accumulating in narrow zones, the existence of shear bands may imply the initiation of material softening as deformation in a shear band proceeds. Such rheological softening will ensure localization of even the most intense shear strains in narrow zones. The velocity will change with time as illustrated in Fig. 1, if the material softens, with localization of strain into narrow zones as time goes on. A laminar flow can be repartitioned to give zones where deformation is essentially coaxial, separated by zones in which the deformation is intensely non-coaxial.

Major movement zones can be described as evolving with space and time through various rheological regimes. Conditions vary spatially, so that major movement zones pass with increasing depth from a zone of faulting and cataclasis to a zone of ductile deformation where mylonites form (Sibson 1977). This has an important influence on the evolution of microstructure, because a particular body of rock is transported with time from one rheological environment to another. A sequence of behaviour which is not uncommon is as follows: (a) a period of penetrative plastic deformation involving large-scale non-coaxial laminar flow; (b) plastic deformation which concentrates in increasingly narrow zones of intense shear strain, leading to the formation of S–C relationships; (c) brecciation and cataclasis, at which stage fault melts may have transient existence, depending on the presence or absence of pore fluid, and on rock composition; (d) formation of (often anastomosing) discrete brittle faults which slice into the previously deformed rocks. This time history has to be considered when discussing the kinematic significance of a group of mylonitic rocks.

CONCLUSIONS

S–C mylonites (of all types) are an important addition to the catalogue of structures and microstructures that can be used to help understand the evolution of complexly deformed bodies of rock. Preliminary investigations suggest that kilometre-scale zones of penetrative non-coaxial laminar flow are more prevalent than currently acknowledged.

There are two types of S–C mylonites commonly found in zones of high shear strain. Type I (reported by Berthé *et al.* 1979) involves shear bands on a scale larger than that of the grain scale, and the mylonitic foliation anastomoses in and out of zones of relatively high shear strain. Type II S–C mylonites involve C-surfaces defined by mica fish trails, caused by displacement discontinuities and microscopic zones of very high shear strain. Oblique foliations are often developed in the adjacent masses of dynamically recrystallized quartz, characterized by grain elongations, alignments of segments of the enveloping surfaces to the grain boundaries, and alignments of families of grains with related orientations. These oblique foliations appear to have been caused by dynamic recrystallization which periodically reset the 'finite-strain clock' as deformation took place.

This study suggests a number of kinematic indicators which can be used to infer the presence of a zone of non-coaxial laminar flow, and the sense of shear in the zone: (a) asymmetric mica 'fish'; (b) asymmetric relations of the mica 'fish' with adjacent trails which consist of mica fragments, recrystallized small grains, and metamorphic reaction products; (c) stair-stepping of the mica 'fish' trails from one mica clast to the next; (d) presence of antithetic 'listric normal faults' or clast shapes with characteristic asymmetry, which indicate the prior existence of such microfaults; (e) presence of various oblique foliations in the dynamically recrystallized quartz masses adjacent to the C-surfaces); (f) S–C relationships in general, as long as only one sense of shear is dominant overall: and (g) asymmetric quartz *c*-axis fabrics.

A broad class of S–C tectonites is proposed. The S-surfaces can be defined by any statistically penetrative foliation, not necessarily a foliation directly related to the accumulation of finite strain. The C-surfaces are defined by zones of intense shear strain or displacement discontinuities. Further, a deviation from the tradition of purely geometric analysis of foliation and time relationships is suggested. With respect to timing relationships, we emphasize that the most relevant question is whether the S–C relationship in a tectonite is a product of ongoing deformation, or simply a coincidental relationship, with shear bands passing through a body of rock which contains other foliations produced during previous epochs of deformation.

Acknowledgements—We acknowledge support of National Science Foundation Grant EAR 8121188. George Davis is thanked for the assistance and encouragement he gave this project. Many of the examples shown in this paper come from the Coyote Mountains, SW of Tucson, Arizona, and we are grateful to Anne Gardulski and

George Davis for allowing us to use this material for illustrative purposes in this paper. Examples from the Betic Cordillera were donated by Reinoud Vissers, and examples from Naxos, Cyclades, Greece, by Olaf Schuiling, University of Utrecht. Specimens from the 'platengneiss' of the Austro-Alpine were collected by courtesy of Prof. W. Frank, University of Vienna, and specimens of the Windy Point gneiss, from the Catalina Mountains, Arizona, by courtesy of Stan Keith, Tucson, Arizona. Discussions with George Davis, Lee DiTullio, Bob Krantz, Elizabeth Miller, John Platt, Steve Reynolds and Reinoud Vissers, helped clarify the concepts presented in this paper.

REFERENCES

Behrmann, J. H. & Platt, J. P. 1982. Sense of nappe emplacement from quartz *c*-axis fabrics; an example from the Betic Cordilleras (Spain). *Earth Planet. Sci. Lett.* **59**, 208–215.

Bell, T. H. & Etheridge, M. A. 1973. Microstructures of mylonites and their descriptive terminology. *Lithos* **6**, 337–348.

Berthé, D., Choukroune, P. & Jegouzo, P. 1979. Orthogneiss, mylonite and non coaxial deformation of granites: the example of the South Amorican Shear-Zone. *J. Struct. Geol.* **1**, 31–42.

Bouchez, J.-L., Lister, G. S. & Nicholas, A. 1983. Fabric asymmetry and shear sense in movement zones. *Geol. Rdsch.* **72**, 401–420.

Bouchez, J.-L. & Pecher, A. 1981. The Himalayan Main Central Thrust pile and its quartz rich tectonites in central Nepal. *Tectonophysics* **78**, 23–50.

Carreras, J., Estrada, A. & White, S. H. 1977. The effects of folding on the *c*-axis fabrics of a quartz mylonite. *Tectonophysics* **39**, 3–24.

Eisbacher, G. H. 1970. Deformation mechanics of mylonite rocks and fractured granites in Cobequid Mountains, Novia Scotia, Canada. *Bull. geol. Soc. Am.* **81**, 2009–2020.

Garcia Celma, A. 1982. Domainal and fabric heterogeneities in the Cap de Creus Quartz mylonites. *J. Struct. Geol.* **4**, 443–456.

Garcia Celma, A. 1983. C-axis and shape fabrics in quartz mylonites of Cap de Creus (Spain); their properties and development. Ph. D. thesis, Insitute of Earth Sciences, University of Utrecht. (Available from library.)

Jegouzo, P. 1980. The South Armorican shear zone. *J. Struct. Geol.* **2**, 39–47.

Higgins, M. W. 1971. Cataclastic rocks. *Prof. Pap. U.S. geol. Surv.* **687**, 1–97.

Law, R. D., Knipe, R. J. & Dayan, H. 1984. Strain path partitioning within thrust sheets: microstructural and petrofabric evidence from the Moine Thrust zone at Loch Eriboll, Northwest Scotland. *J. Struct. Geol.* **6**, 477–497.

Lister, G. S. & Hobbs, B. E. 1979. The simulation of fabric development during plastic deformation and its application to quartzite: the influence of deformation history. *J. Struct. Geol.* **1**, 283–297.

Lister, G. S. & Dornsiepen, U. F. 1980. Fabric transitions in the Saxony Granulite terrain. *J. Struct. Geol.* **4**, 81–92.

Lister, G. S. & Williams, P. F. 1979. Fabric development in shear zones: theoretical controls and observed phenomena. *J. Struct. Geol.* **1**, 283–297.

Lister, G. S. & Williams, P. F. 1983. The partitioning of deformation in flowing rock masses. *Tectonophysics* **92**, 1–34.

Means, W. D. 1981. The concept of steady state foliation. *Tectonophysics* **78**, 179–199.

Means, W. D., Hobbs, B. E., Lister, G. S. & Williams, P. F. 1980. Vorticity and non-coaxiality in progressive deformations. *J. Struct. Geol.* **2**, 371–378.

Paterson, M. S. & Weiss, L. E. 1961. Symmetry concepts in the structural analysis of deformed rocks. *Bull. geol. Soc. Am.* **72**, 841–882.

Platt, J. P. & Vissers, R. L. M. 1980. Extensional structures in anisotropic rocks. *J. Struct. Geol.* **2**, 397–410.

Poirier, J.-P. & Nicholas, A. 1975. Deformation-induced recrystallization due to progressive misorientation of subgrains, with special reference to mantle peridotites. *J. Geol.* **83**, 707–720.

Poirier, J.-P., & Guillopé, M. 1978. Deformation induced recrystallization of minerals. *Bull. Soc. fr. Minér. Cristallogr.* **102**, 67–74.

Ponce de Leon, M. I. & Choukroune, P. 1980. Shear zones in the Iberian Arc. *J. Struct. Geol.* **2**, 63–68.

Sibson, R. H. 1975. Generation of pseudotachylite by ancient seismic faulting. *Geophys. J. R. astr. Soc.* **43**, 775–794.

Sibson, R. H. 1977. Fault rocks and fault mechanisms. *J. geol. Soc. Lond.* **133**, 191–213.

Simpson, C. & Schmid., S. M. 1983. Microstructural indicators of sense of shear in shear-zones. *Bull. geol. Soc. Am.* **94**, 1281–1288.

Snoke, A. W. 1980. Transition from infrastructure to suprastructure in the northern Ruby Mountains, Nevada. In: Cordilleran Metamorphic Core Complexes (edited by Crittenden, M. D., Jr. *et al.*). *Mem. geol. Soc. Am.* **153**, 287–333.

Sylvester, A. G. & Christie, J. M. 1968. The origin of crossed-girdle orientations of optic axes in deformed quartzites. *J. Geol.* **76**, 571–580.

Sylvester, A. G., Oertel, G., Nelson, C. A. *et al.* 1978. Papoose Flat Pluton; a granitic blister in the Inyo Mountains, California. *Bull. geol. Soc. Am.* **89**, 1205–1219.

Thorman, C. H. 1981. Geology of the Pinaleno Mountains, Arizona. A preliminary report. *Ariz. geol. Soc. Digest* **13**, 5–112.

Urai, J. L. 1983. Deformation of wet salt rocks: an investigation into the interaction between mechanical properties and microstructural processes during deformation of polycrystalline carnallite and bischofite in the presence of a pore fluid. Ph.D. thesis, Institute for Earth Sciences, University of Utrecht. (Available from library.)

Vernon, R. H., Williams, V. A. & D'Arcy, W. F. 1983. Grain size reduction and foliation development in a deformed granite batholith. *Tectonophysics* **92**, 123–146.